Human Cerebral Cortex: Localization, Parcellation, and Morphometry with Magnetic Resonance Imaging

J. Rademacher, A. M. Galaburda, D. N. Kennedy, P. A. Filipek, and V. S. Caviness, Jr.
Harvard Medical School

Abstract

■ We describe a system of parcellation of the human brain that is based on the functional anatomy of the cerebral cortex and that is applied to the analysis of magnetic resonance images. This system is designed to support investigations of hemispheric asymmetries and quantitative lesion localization studies in cognitive neuroscience. The system of cortical subdivision is a neural systems oriented model that approximates subdivisions supported by previous architectonic and functional analyses. It is based primarily on boundaries determined by "limiting fissures." It is completed by a set of coronal planes, keyed to visible anatomic landmarks, which "close" the borders of the parcellation subdivisions. The method depends on computational reconstruction of the primary image data in multiple planes so as to allow the observed pattern of limiting fissures in a given brain to be digitized. In this presentation, the method is applied in order to define the surface anatomy of the cerebral hemispheres in a normal subject. Volumetric measurements of individual cortical regions are compared as hemispheric percentiles to areal percentiles derived from the analysis of Jouandet et al. (1989), a conceptually related though methodologically different approach. We specifically address the approach to the study of interhemispheric differences and interindividual variations in cortical anatomy. ■

INTRODUCTION

Because the question of how function maps onto structure is of central interest in cognitive neuroscience, the precision of anatomical measures is an important methodological issue. High-resolution magnetic resonance imaging (MRI) achieves precise in vivo visualization of specific anatomical landmarks and lesions. It is of unique value for the assessment of individual anatomical variations and left–right asymmetries (Steinmetz et al., 1989b, 1990c) of functional relevance (Geschwind & Levitsky, 1968; Galaburda, Sanides, & Geschwind, 1978; Galaburda, Sherman, Rosen, Aboitiz, & Geschwind, 1985; Geschwind & Galaburda, 1985; Steinmetz, Volkmann, Jäncke, & Freund, 1991). The application of volumetric morphometric techniques (Filipek et al., 1989) provides increased sensitivity of measure in comparison to earlier CT or MRI studies limited to the measurement of linear parameters or cortical areas on a single image plane (LeMay & Kido, 1978; Habib, Renucci, Vanier, Corbaz, & Salamon, 1984; Pieniadz & Naeser, 1984; Kertesz, Black, Polk, & Howell, 1986). Morphometric studies of in vivo brain anatomy using MR also have the advantage that they are free of the variations in brain morphology inevitable with terminal illness, postmortem autolysis, and tissue processing for histology.

The consistent definition of functionally relevant regions is a precondition for localization and morphometry. There are three modern approaches to this problem. The stereotactic proportional grid of Talairach (Talairach et al., 1967) is frequently used as an indirect reference system (Fox, Perlmutter, & Raichle, 1985; Fox et al., 1986; Fox, Burton, & Raichle, 1987; Perlmutter, Powers, Herscovitch, Fox, & Raichle 1987; Petersen, Fox, Posner, Mintun, & Raichle, 1988; Posner, Petersen, Fox, & Raichle, 1988; Petersen, Fox, Snyder, & Raichle, 1990; Chollet et al., 1991; Corbetta, Miezin, Dobmeyer, Shulman, & Petersen, 1991; Wise et al., 1991). It defines spatial coordinates for brain gyri, brain sulci, and cytoarchitectonic fields. A second approach is based on template overlays (Gelbert et al., 1986; Damasio & Damasio, 1989), which can be integrated into standardized computerized brain atlases (Bajcsy, Lieberson, & Reivich, 1983; Bohm, Greitz, Kingsley, Berggren, & Olsson, 1983; Evans, Beil, Marrett, Thompson, & Hakim, 1988; Dann, Hoford, Kovacic, Reivich, & Bajcsy, 1989; Seitz et al., 1990; Greitz, Bohm, Holte, & Eriksson, 1991). For the critical identification of the individual anatomical pattern, both methods rely on normative descriptors for a standard brain. The wide range of interindividual and interhemispheric morphological differences (Eberstaller, 1890; Cunningham, 1892; Retzius, 1896; Bailey & von Bonin, 1951; Lang & Wach-

© 1992 Massachusetts Institute of Technology

smuth, 1985; Ono, Kubik, & Abernathey, 1990) cannot be compensated for by these methods (Steinmetz, Fürst, & Freund, 1989a; Steinmetz, Fürst, & Freund, 1990b).

A third method parcellates the hemispheric surface on the basis of the topography of individual gyri and sulci (Jouandet et al., 1989) and therefore deals directly with the substantial variability. It takes advantage of the relationship between "limiting sulci" and cytoarchitectonic field boundaries (Sanides, 1962). Additionally, it differentiates between the intrasulcal and exposed brain surface. Despite these advantages, this approach is limited in that it offers no explicit guide to the definition of individual gyri and sulcal topography. Visible sulcal landmarks are not sufficient for a complete parcellation of the human brain into functionally relevant compartments. Also, a substantial subset of the sulci are not reliably delineated in the coronal plane alone.

The present method builds on the strengths of the technique proposed by Jouandet et al. (1989), but also provides solutions to its limitations, which will make it applicable by other investigators. We provide a neural systems approach to the parcellation of the human brain that is based on sulcal landmarks and complementary anatomic conventions. The system is hierarchical with subdivision into primary sensory and motor areas, unimodal and heteromodal association areas, and paralimbic and limbic regions (Flechsig, 1920; Mesulam, 1985; Pandya & Yeterian, 1985). The relationship of cytoarchitectonic subdivisions to these surface maps is considered

Brodmann, 1909; von Economo & Koskinas, 1925; Sanides, 1962; Braak, 1980).

RESULTS

Neural Systems Model of Parcellation

We have adopted a system of parcellation of the human cerebral cortex that is based on current views of the functional organization of the primate (human and nonhuman) brain (Figs. 1 to 6). An overview and rationale for this model will be considered in the discussion.

Localization and Parcellation

The keystone to our parcellation method are the "limiting fissures" of the cerebrum. This relatively constant set of brain sulci guides our approach. The coronal plane was chosen as a starting point and reference plane. At first, those sulci or sulcal segments that were readily identified on the standard coronal plane were marked. Those that could not be identified in the coronal plane because of their orientation, discontinuity, or otherwise atypical configuration were subsequently identified in the sagittal or transaxial planes, and their outlines were transferred to the coronal image sequence (Figs. 7, 8, and 9). Because of the curvature of the brain, not every sulcus can be marked over its complete course on one single slice. Consequently, the full extent of these sulci was determined by the analysis of a sequence of images. Because the course of certain brain sulci critical to the parcellation may be interrupted, the method requires that the missing segments of these sulci be edited in by tracing bridges across gyral surfaces.

The "limiting sulci" of the human brain are not sufficient to provide complete boundaries for every region of interest. We have addressed this deficiency, inherent to any fissure-based parcellation method, by defining a set of anatomic conventions. The open contours of a specific compartment were closed at the level of a constant coronal plane. (In transition across this coronal plane, the algorithm is signaled to construct a boundary.) Each "limiting coronal plane," with a single exception, was defined consistently by a nodal point in the cerebral surface anatomy (e.g., coronal plane D in Fig. 1B is defined by the posterior end of the sylvian fissure).

Sulcal Anatomy of the Lateral Cerebral Surface

The limiting sulci of the lateral cerebral surface are depicted in Figures 1 and 2.

Frontal Lobe

Central Sulcus. The central sulcus has a characteristic continuous course (Fig. 1A) from a dorsocaudal point at the vertex to an anteroventral point near the superior lip of the sylvian fissure (Eberstaller, 1890). Variably [60% (Cunningham, 1892) to 88% (Lang & Wachsmuth, 1985)] it extends onto the dorsomedial brain surface (Fig. 3A). Its upper segment is identified in the transaxial plane where it is interposed between the precentral and postcentral sulci. The inferior part of the central sulcus is optimally identified in the sagittal plane, as the sulcus posterior to the inferior precentral sulcus.

Precentral Sulcus. The precentral sulcus follows a dorsomedial to ventrolateral course that is rostral and roughly parallel to the central sulcus. It is intersected orthogonally by the superior and inferior frontal sulci (Fig. 2). Variably it continues onto the medial brain surface, where it limits the paracentral lobule anteriorly (Eberstaller, 1890). The inferior part of the precentral sulcus lies behind the anterior ascending ramus of the sylvian fissure (Fig. 1A). Duplication of the ventrolateral segment is a common variant (Ono et al., 1990). As with the central sulcus, the characteristic topographical patterns are optimally identified in the transaxial plane for the superior segment and in the sagittal plane for the inferior segment.

Superior and Inferior Frontal Sulci. Throughout the frontal lobe the superior and inferior frontal sulci follow a course parallel to each other and to the interhemis-

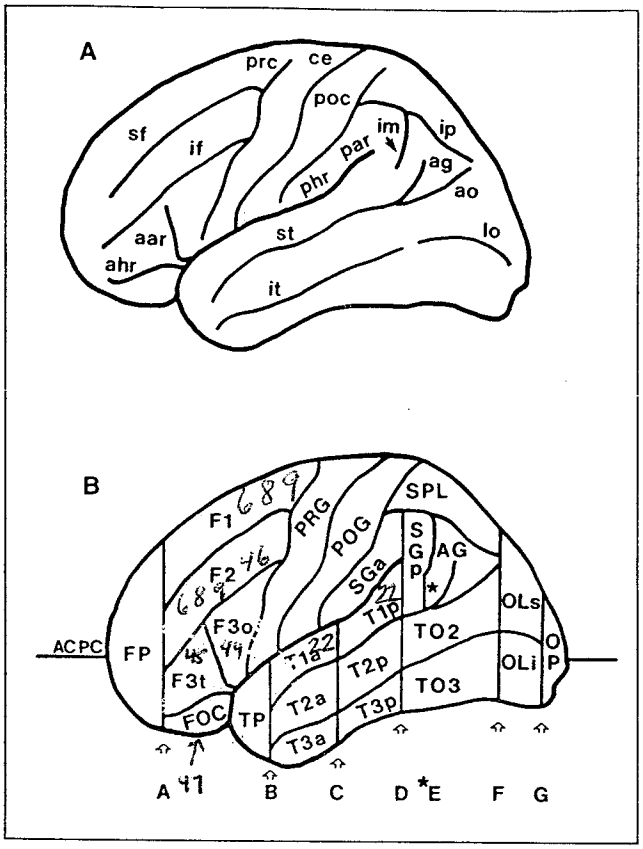

Figure 1. Schematic drawings of the lateral cerebral surface (left hemisphere) with cortical parcellation units, limiting sulci and coronal planes. (See Table 1 for key to sulcal abbreviations and Table 2 for definition and key to abbreviations of the parcellation units.) (A) Idealized topography of the limiting sulci. (B) Idealized topography of the cortical parcellation units. Coronal planes A to G are defined by the AC–PC (anterior commissure–posterior commissure) line and individual cerebral landmarks (see Results). The intersections of both specific sulci and coronal planes create closed regions of interest. Only those coronal planes are shown which are applied to specific parcellation units of the lateral convexity (see Figs. 2 to 6 for the dorsal, medial, ventral, and intrasylvian surfaces).

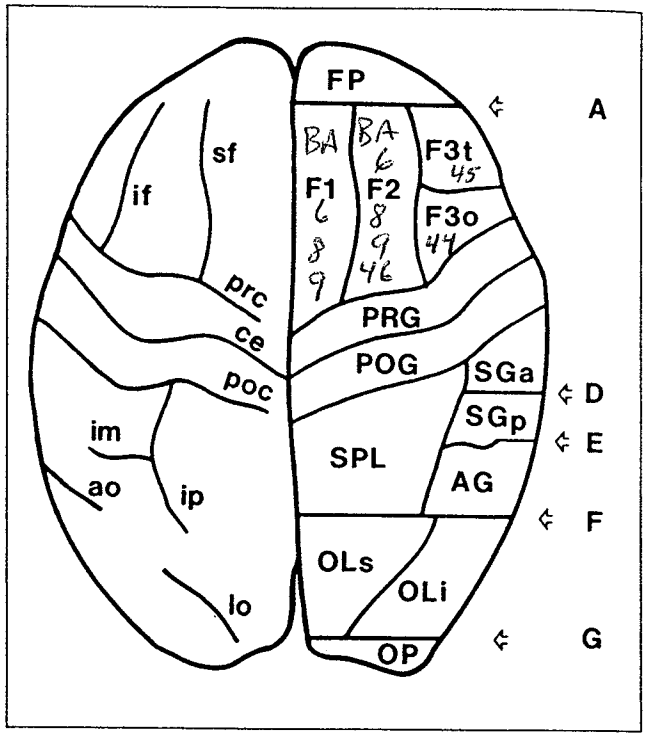

Figure 2. Schematic drawing of the dorsal cerebral surfaces with cortical parcellation units, limiting sulci and coronal planes (A, D to G). The dorsal view illustrates the cerebral topography as shown in Figure 1. It does not introduce new structures. On the left side (left hemisphere; anterior is at the top) the idealized topography of the limiting sulci is depicted. On the right side the idealized topography of the cortical parcellation units is shown. Coronal planes B and C are not visible because they are applied exclusively to the temporal lobe. (See Tables 1 and 2 for key to abbreviations.)

pheric plane (Fig. 2). Posteriorly both meet the precentral sulcus at right angles. This conjunction aids in the delineation of both the superior and inferior frontal sulci as well as the precentral sulcus. The inferior frontal sulcus lies dorsal to the frontal operculum (Fig. 1B). The course of the superior frontal sulcus is optimally identified in the transaxial plane and that of the inferior frontal sulcus in the sagittal plane.

Anterior Ascending and Anterior Horizontal Rami of the Sylvian Fissure. The most rostral segments of the sylvian fissure, the anterior ascending and horizontal rami, radiate from a point immediately anterior to the inferior precentral sulcus (Fig. 1A). They subdivide the frontal operculum (Fig. 1B) into its posterior pars opercularis, intermediate pars triangularis, and anterior pars orbitalis (Eberstaller, 1890). Alternatively the diagonal sulcus (not shown), lying posteriorly to the anterior ascending ramus, may represent the border between the posterior and intermediate segments. The sagittal plane provides optimal visualization of the transfrontal course of these sulci.

Temporal Lobe

Posterior Horizontal Ramus of the Sylvian Fissure. The sylvian fissure is the dominant fissure of the lateral hemisphere and is unique for its great depth. Leftward asymmetry of the sylvian fissures is the rule in at least 69% of human brains (Rubens, Mahowald, & Hutton, 1976). The main trunk, the posterior horizontal ramus (Fig. 1A), is bordered inferiorly by the supratemporal plane and superiorly by the frontal and parietal opercula. Rostrally it gives rise to the anterior ascending and horizontal rami while caudally the posterior ascending ramus is the main branch. The full course of the sylvian fissure is optimally visualized in the sagittal plane (Steinmetz et al., 1990b).

Posterior Ascending Ramus of the Sylvian Fissure. The posterior ascending ramus represents the axis of the supramarginal gyrus (Fig. 1A). Its presence (left: 44%, right: 92%; Ono et al., 1990) and extent are decisive

determinants of the interhemispheric asymmetries described above (Steinmetz et al., 1990c). Its upward anoulation is optimally visualized in the sagittal plane.

Superior Temporal Sulcus, Angular Sulcus, and Anterior Occipital Sulcus. The trunk of the superior temporal sulcus runs parallel to the sylvian fissure (Fig. 1A) and defines the inferior border of the superior temporal gyrus. Anteriorly it ends close to the temporal pole. Posteriorly, the superior temporal sulcus gives rise to the angular sulcus and the anterior occipital sulcus (Bailey & von Bonin, 1951; Ono et al., 1990). Caudal and parallel to the posterior ascending ramus of the sylvian fissure, the angular sulcus is axial to the angular gyrus (Fig. 1A). Posterior to the angular gyrus, the anterior occipital sulcus arches dorsally. The superior temporal sulcus and its branches are optimally visualized in the sagittal plane.

Inferior Temporal Sulcus. The inferior temporal sulcus, though parallel to the superior, does not extend as far toward the temporal tip. It is typically interrupted and in many brains extends onto the ventral cerebral surface (Lang & Belz, 1981). Posteriorly, it is frequently continuous with the lateral occipital sulcus. Variant courses are continuous with the anterior occipital sulcus (Ono et al., 1990). The inferior temporal sulcus is distinguished optimally in the sagittal and coronal planes.

Parietal Lobe

Postcentral Sulcus. The postcentral sulcus lies posterior to the central sulcus, which it parallels approximately, from the dorsal hemispheric margin to the sylvian fissure (Figs. 1A and 2). It is frequently discontinuous. Its dorsal segment is intersected at an acute angle by the intraparietal sulcus (Fig. 2). The inferior segment lies typically between the inferior central sulcus and the posterior ascending ramus of the sylvian fissure (Steinmetz, Ebeling, Huang, & Kahn, 1990a). As a common variant (left: 16%, right: 8%), the inferior segment may be parallel to the anterior part of the intraparietal sulcus (Ono et al., 1990). The dorsal segment often (80%) has a terminally bifurcated Y-shaped configuration at the hemispheric margin, with the marginal ramus of the cingulate sulcus lying between the terminal forks. The dorsal segment (Fig. 2) is optimally visualized in the transaxial plane and the inferior segment (Fig. 1A) in the sagittal plane.

Intraparietal Sulcus. The deep and opercularizing intraparietal sulcus follows an approximately transaxial course which partitions the superior and inferior parietal lobules (Fig. 2). Rostrally, the relationship to the postcentral sulcus is characteristic (Cunningham, 1892; Retzius, 1896). Although of variable length and configuration (Bailey & von Bonin, 1951) the intraparietal sulcus typically (98%) extends slightly into the occipital lobe (Ono et al., 1990). The intraparietal sulcus is optimally visualized in the transaxial plane.

Intermediate Sulcus of Jensen. The intermediate sulcus is a downward-projecting side branch of the intraparietal sulcus (Fig. 1A). It descends across the inferior parietal lobule and separates the supramarginal from the angular gyrus (Figs. 1B and 2). It may continue far enough to intersect the superior temporal sulcus (Ono et al., 1990). It is optimally visualized in the sagittal plane.

Occipital Lobe

Lateral Occipital Sulcus. The lateral occipital sulcus runs horizontally across the occipital lobe (Fig. 1A) and delineates superior and inferior occipital gyri (Figs. 1B and 2). Present in 96% of brains (Ono et al., 1990), it is an exception to the rule that there are no constant sulci on the lateral occipital surface (Bailey & von Bonin, 1951). The lateral occipital sulcus is optimally visualized in the sagittal plane.

Sucal Anatomy of the Medial Cerebral Surface

The structures of the medial brain surface are generally best visualized in the sagittal plane. The limiting sulci of the medial cerebral surface are depicted in Figure 3.

Frontal Lobe

Superior Rostral Sulcus. The superior rostral sulcus (Fig. 3A) ascends radially from the anterior subcallosal region and extends toward the anterior hemispheric margin (Eberstaller, 1890). It is paralleled by the shallow and less frequent inferior rostral sulcus (not shown).

Cingulate and Paracingulate Sulci. The cingulate sulcus follows a course parallel to the corpus callosum (Fig. 3A). Its posterior terminal branch is the marginal sulcus. Anteriorly it arches over the genu of the corpus callosum. The paracingulate sulcus lies just in front of and parallel to the anterior part of the cingulate sulcus (Fig. 3A).

Marginal Sulcus. The marginal sulcus is directly continuous with the cingulate sulcus (Fig. 3A). It courses upward and reaches the dorsomedial hemispheric margin. In the majority of brains (98%) it terminates at a point immediately posterior to the central sulcus (Ono et al., 1990).

Callosal Sulcus. The callosal sulcus defines the margin of the corpus callosum with cortex throughout the full extent of the commissure. For convenience it is listed here together with the sulci of the frontal lobe.

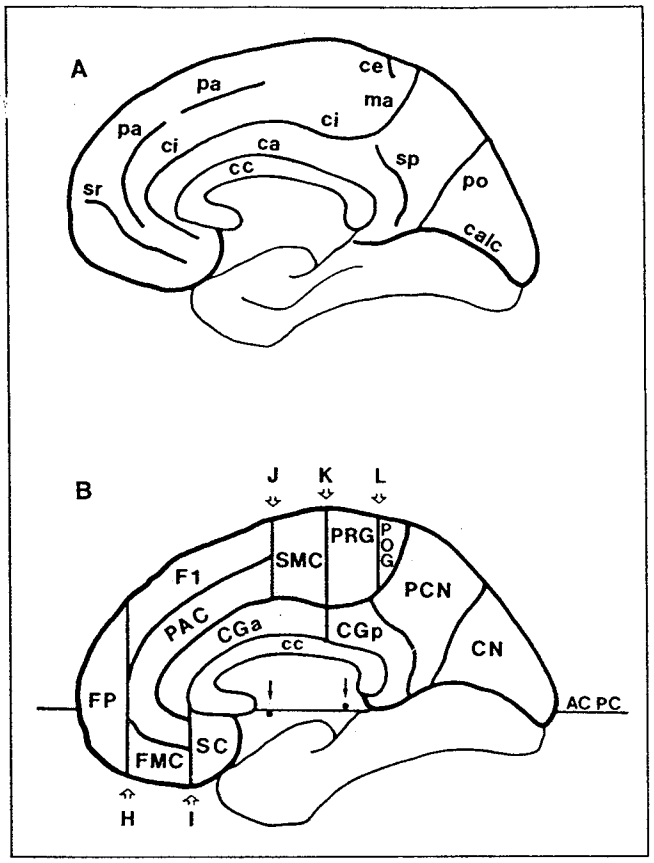

Figure 3. Schematic drawings of the medial cerebral surface (right hemisphere) with cortical parcellation units, limiting sulci and coronal planes. (See Tables 1 and 2 for key to abbreviations.) (A) Idealized topography of the limiting sulci. (B) Idealized topography of the cortical parcellation units. Coronal planes H to L are depicted. (Solid arrows), anterior and posterior commissures. (AC PC), bicommissural plane (tangent to the upper margin of the anterior commissure and to the lower margin of the posterior commissure).

Parietal Lobe

Subparietal Sulcus. The main segment of the subparietal sulcus follows a course parallel to the corpus callosum (Fig. 3A), separating the precuneus from the cingulate gyrus (Fig. 3B). Anteriorly it originates at the point of the upward angulation of the marginal sulcus, where it is frequently (32%) confluent with the cingulate sulcus (Ono et al., 1990). Posteriorly it extends toward the anterior part of the calcarine sulcus.

Parietooccipital Sulcus. The parietooccipital sulcus follows a typical course from a dorso-caudal point at the hemispheric margin, to an anteroventral point at the junction with the calcarine sulcus (Fig. 3A). It is distinguished by its great depth and its topographical relationship to the calcarine sulcus.

Occipital Lobe

Calcarine Sulcus. The calcarine sulcus extends from the occipital pole to a point just below and anterior to the splenium of the corpus callosum (Fig. 3A and B). Its anterior segment separates the isthmus of the cingulate gyrus and the parahippocampal gyrus from the lingual gyrus. Its conjunction with the parietooccipital sulcus at a point caudal to the splenium ("cuneal point"; Fig. 8A) is a principal landmark of the medial hemispheric surface.

Temporal Lobe

Our definition of the medial brain surface includes only the structures that are visualized on the midsagittal plane with MRI (Fig. 3A and B). The sulci of the medial temporal lobe will be described together with those of the ventral temporal lobe.

Sulcal Anatomy of the Ventral Cerebral Surface

On the ventral brain surface the sulci are optimally visualized in the coronal plane. As an exception of the rule, the transverse orbital sulcus is optimally visualized in the sagittal plane. The limiting sulci of the ventral cerebral surface are depicted in Figure 4.

Frontal Lobe

Olfactory Sulcus. The olfactory sulcus, lying just lateral to the medial hemispheric margin, follows a parasagittal course. It is a constant (100%) landmark (Ono et al., 1990).

Medial and Transverse Orbital Sulci. The medial orbital sulcus follows a course parallel to the olfactory sulcus. The transverse orbital sulcus courses transversely across the ventral brain surface. It is the most constant (88–100%) sulcus of the orbital group (Eberstaller, 1890; Ono et al., 1990).

Temporal and Occipital Lobes

Occipitotemporal Sulcus. The occipitotemporal sulcus follows an approximately parasagittal course just medial to the inferolateral margin of the hemisphere. Rarely (6%), it is "duplicated" through part of its course (not shown; Ono et al., 1990). In this case the lateral branch separates the inferior temporal and fusiform gyri.

Collateral Sulcus. The collateral sulcus courses along the ventro-medial surface of the temporal and occipital lobes. It follows closely the parahippocampal gyrus anteriorly and the lingual gyrus posteriorly (Naidich et al., 1987). The caudal collateral sulcus is frequently (48%)

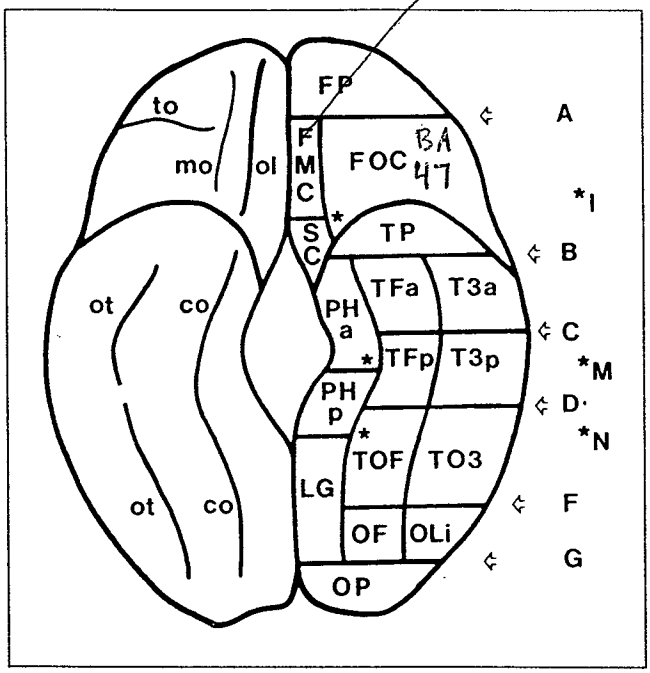

Figure 4. Schematic drawing of the ventral cerebral surfaces with cortical parcellation units, limiting sulci and coronal planes (A to D, F, G, I, M, N). On the left side (right hemisphere) the idealized topography of the limiting sulci is depicted. On the right side the idealized topography of the cortical parcellation units is shown. Not all of the coronal planes are applied to structures of the ventral cerebral surfaces. Therefore their appearance in the rostro-caudal direction is not alphabetical. (See Tables 1 and 2 for key to abbreviations.)

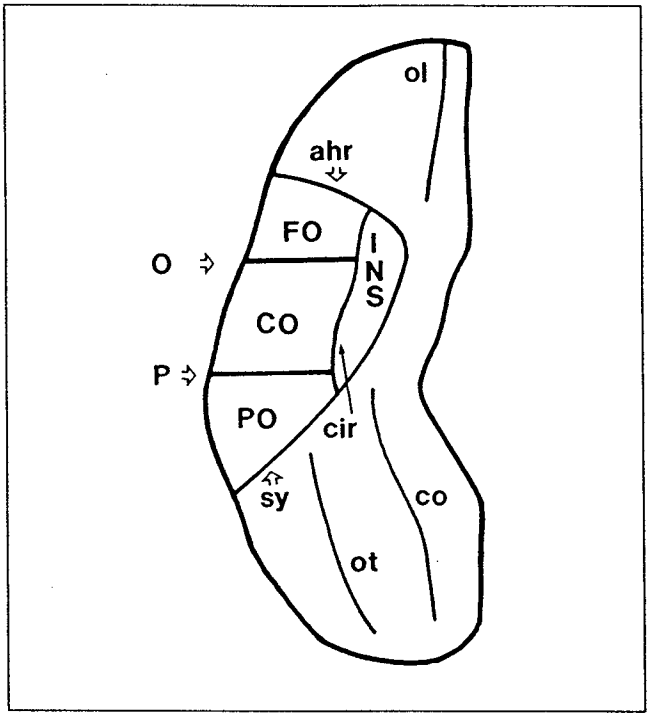

Figure 5. Schematic drawing of the intrasylvian surface of the frontoparietal operculum (view from below of the right hemisphere; anterior is at the top) with cortical parcellation units, limiting sulci, and coronal planes (O, P). With the temporal lobe and parts of the frontal lobe being removed, the idealized representation shows the total anterior–posterior extent of the sylvian fossa. (See Tables 1 and 2 for key to abbreviations.)

bifurcated (Ono et al., 1990). In this case the medial branch represents the intralingual sulcus (not shown), while the lateral ramus separates the lingual and fusiform gyri.

Hippocampal Fissure. The hippocampal fissure (Fig. 9A) separates the parahippocampal gyrus from the hippocampus proper, which is located dorsally (Duvernoy, 1988). Ventrally, the subicular complex forms part of the parahippocampal gyrus.

Sulcal Anatomy of the Intrasylvian Cerebral Surface

Frontoparietal Operculum

There are no reliable sulcal landmarks on the intrasylvian extent of the frontoparietal operculum (Fig. 5).

Temporal Operculum

The superior temporal surface is depicted in Figure 6.

Circular Sulcus of the Insula. The circular sulcus, lying in the depth of the sylvian fossa, is defined throughout its circumference by the origins of the perisylvian opercula. It is optimally visualized in the sagittal plane.

First Transverse Sulcus. The first transverse sulcus is the sulcus lying just in front of and parallel to Heschl's gyrus, which is the anteriormost transverse gyrus on the posterior supratemporal plane (Pfeifer, 1920, 1936).

Heschl Sulcus. The Heschl sulcus is the diagonal sulcus immediately behind the prominent Heschl gyrus. Its continuous course is visualized in the transaxial plane (Steinmetz et al., 1989b). The sagittal and coronal planes provide optimal visualization of the variable courses of the transverse gyri.

Coronal Planes

A set of 16 coronal [defined by X and Z axes of Talairach et al., (1967)] planes (designated by capital letters, A to P) defines the complementary boundaries needed for parcellation and not provided by limiting fissures (Figs. 1B, 2, 3B, 4, 5, and 6). The position of each of these planes along the *Y* axis is defined, with one exception (coronal plane G), by the location of recognizable, constant landmarks or "nodal points" in the cerebrum that have been found to be related to functionally relevant boundaries (see Discussion). For example, coronal plane F (Figs. 1B and 2) is defined by the point where the parietooccipital sulcus cuts into the dorsal hemispheric

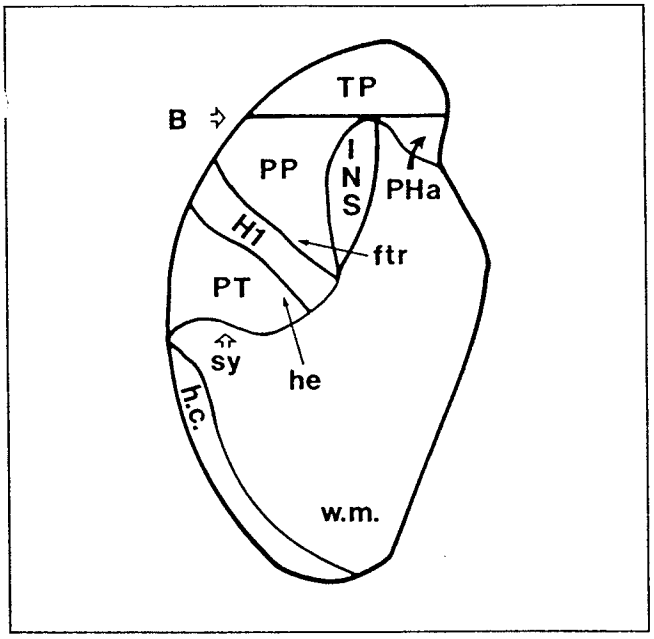

Figure 6. Schematic drawing of the intrasylvian surface of the supratemporal plane (view from above of the left hemisphere; anterior is at the top) with cortical parcellation units, limiting sulci, and coronal plane B. The circular sulcus (not labeled) defines the circumference of the insula. The frontal and parietal lobes have been removed by a transverse cut along the sylvian fissure. Abbreviations: h.c., hemispheric convexity of the parietal lobe; w.m., white matter in the sectional plane. (See Tables 1 and 2 for key to abbreviations.)

margin (Fig. 3A). The nodal points are listed in the following section. Associated parcellation units are mentioned to facilitate the understanding of the topographic relations. The complete parcellation system and its boundaries are summarized in Figures 1 to 6 and in Table 2. It can be seen in Figures 1 to 6 that a given "limiting coronal plane" defines the boundaries of only a small (specific) set of parcellation units. The intersections of limiting sulci and coronal planes A to P create complete (closed) units for morphometry. The planes are labeled topographically according to the location of their nodal points: planes A–G on the lateral, H–L on the medial, M and N on the ventral, and O and P on the intrasylvian brain surfaces. This does not mean that individual coronal planes do not extend across more than one surface.

Lateral Cerebral Surface

Coronal plane A is defined by the rostral end of the anterior horizontal ramus of the sylvian fissure (Fig. 1B). It serves as the posterior boundary of the frontal pole on the lateral (Figs. 1B and 2) and ventral (Fig. 4) brain surfaces.

Coronal plane B, the anterior–posterior axis considered, is defined as the first coronal slice that contains the temporofrontal junction. It represents the caudal border of the temporal pole (Figs. 1B, 4, and 6).

Table 1. Key to Sulcal Abbreviations, Listed Topographically.[a]

Lateral Cerebral Surface	
Frontal lobe	
ce	central sulcus
prc	precentral sulcus
sf	superior frontal sulcus
if	inferior frontal sulcus
aar	anterior ascending ramus of sy
ahr	anterior horizontal ramus of sy
sy	Sylvian fissure (total extent)
Temporal lobe	
phr	posterior horizontal ramus of sy
par	posterior ascending ramus of sy
st	superior temporal sulcus
it	inferior temporal sulcus
Parietal lobe	
poc	postcentral sulcus
ip	intraparietal sulcus
im	intermediate sulcus of Jensen
ag	angular sulcus
ao	anterior occipital sulcus
Occipital lobe	
lo	lateral occipital sulcus
Medial Cerebral Surface	
Frontal lobe	
sr	superior rostral sulcus
pa	paracingulate sulcus
ci	cingulate sulcus
ca	callosal sulcus
ma	marginal ramus of ci
Parietal lobe	
sp	subparietal sulcus
po	parietooccipital sulcus
Occipital lobe	
calc	calcarine sulcus
Ventral Cerebral Surface	
Frontal lobe	
mo	medial orbital sulcus
ol	olfactory sulcus
to	transverse orbital sulcus
Temporal and occipital lobes	
hi	hippocampal fissure
co	collateral sulcus
ot	occipitotemporal sulcus
Intrasylvian Cerebral Surface	
cir	circular sulcus of the insula
ftr	first transverse sulcus
he	Heschl sulcus

[a]The abbreviations are also shown in the schematic templates of the limiting sulci in Figures 1 to 6 and they are listed in Table 2 for the definition of the parcellation units.

Coronal plane C is defined by the rostrolateral end of the first transverse sulcus. It subdivides the superior, middle, and inferior temporal gyri (Fig. 1B) as well as the temporal part of the fusiform gyrus (Fig. 4) into anterior and posterior segments.

Coronal plane D is defined by the endpoint of the sylvian fissure (Fig. 1B). It is the anterior border of the occipitotemporal transition zone on the lateral (Figs. 1B and 2) and ventral (Fig. 4) brain surfaces.

Coronal plane E is defined by the inferior end of the intermediate sulcus of Jensen (Fig. 1B). When no intermediate sulcus is present, coronal plane E is taken to lie halfway between the posterior end of both the sylvian fissure (coronal plane D) and the angular sulcus. It separates the supramarginal and angular gyri (Figs. 1B and 2).

Coronal plane F is defined by the point where the parietooccipital sulcus cuts into the dorsal hemispheric margin. Above the intraparietal sulcus it represents the border between the superior parietal and occipital cortices (Fig. 2). Below this level it defines the posterior border of the inferior parietal areas (Fig. 2). Inferior to the superior temporal sulcus it is the caudal border of the temporooccipital transition zone (Fig. 1B).

Coronal plane G is defined as the coronal slice that delineates the caudal 10% of the *Y* axis (Talairach et al., 1967) extent through the hemisphere. It is the only boundary defining plane which is not keyed to a visible anatomic landmark. It defines the boundary of the occipital pole on the lateral and ventral brain surfaces (Figs. 1B, 2, and 4).

Medial Cerebral Surface

Coronal plane H is defined by the anterior tip of the cingulate sulcus (Fig. 3B) and represents the posterior border of the frontal pole medially.

Coronal plane I is defined by the anterior tip of the genu of the corpus callosum (Fig. 3B). It is the border between the subcallosal region posteriorly and the frontomedial cortex anteriorly (Figs. 3B and 4).

Coronal plane J is defined by the anterior commissure (Fig. 3B). As with coronal planes G and M, plane J is, therefore, keyed to nonneocortical landmarks. It represents the posterior border of the paracingulate region and the rostral part of the superior frontal gyrus.

Coronal plane K is defined by the dorsal end of the precentral sulcus (Fig. 3B). It is applied to the cingulate gyrus, which it divides into an anterior and posterior segment. It also separates the supplementary motor cortex from the medial portion of the precentral gyrus.

Coronal plane L is defined by the dorsal end of the central sulcus (Fig. 3B) and divides the paracentral lobule into both an anterior (frontal) and a posterior (parietal) portion, which are continuous with the precentral and postcentral gyri, respectively.

Ventral Cerebral Surface

Coronal plane M is defined as the first coronal slice in the anterior–posterior axis that contains the lateral geniculate nucleus (Fig. 4). It divides the parahippocampal gyrus into an anterior and posterior portion.

Coronal plane N is defined by the anterior end of the calcarine sulcus (Fig. 4). It represents the boundary between the posterior parahippocampal gyrus and the lingual gyrus.

Intrasylvian Cerebral Surface

Coronal plane O is defined by the inferior end of the precentral sulcus at the sylvian fissure (Fig. 5). It separates frontal and central opercula.

Coronal plane P is defined by the inferior end of the postcentral sulcus at the sylvian fissure (Fig. 5). It separates central and parietal opercula.

Morphometry

The regions of interest have been identified and marked on the coronal slices, either directly or by use of the "point-to-point" transfer program. On each slice any selected unit consists of a cortical volume (area × slice thickness) defined by the boundaries of the parcellation system, both limiting sulci and coronal planes, and by the underlying white matter. Once the regions were digitized and labeled for the whole brain, their absolute volumes (Table 4) were computed as the sum of voxels assigned to that unit throughout the coronal series multiplied by the volume equivalent of one voxel in cubic centimeters (Filipek et al., 1989). The volumes of the individual parcellation units range from 1 to 28 cm^3, with most of the values representing less than 5% of the total cortical volume of each hemisphere. With asymmetry being defined as any side difference larger than 10%, 32 parcellation units of a total of 47 (68%) were asymmetric. In contrast, the values for the cerebral lobes (frontal, temporal, etc.) showed symmetry.

We also measured the amount of cerebral cortex that is buried within the depth of the sylvian, intraparietal, and calcarine sulci, independent of the rest of our measurements (Table 4).

DISCUSSION

Our approach to cerebral parcellation provides a neural systems oriented subdivision of the entire human cortex. It relies primarily on the course of "limiting fissures" for boundary delineation. These are the only intrinsic landmarks that support a reproducible parcellation of the surface anatomy of the cerebral hemispheres. We com-

Table 2. Definition of the Borders of the Cortical Parcellation Units.[a]

Parcellation unit	*Anterior border*	*Posterior border*	*Ventral border*	*Dorsal border*
Lateral Surface				
Frontal lobe				
FP, frontal pole[b]	h.m.	A, *H*	—	—
F1, superior frontal gyrus[c]	A, *H*	prc, *J*	sf	*pa*
F2, middle frontal gyrus	A	prc	if	sf
F3t, inferior frontal gyrus/pars triangularis	A	aar	ahr	if
F3o, inferior frontal gyrus/pars opercularis	aar	prc	phr	if
PRG, precentral gyrus[c]	prc, *K*	ce, *L*	phr	*ci*
Temporal lobe				
TP, temporal pole[a]	h.m.	B	—	—
T1a, superior temporal gyrus/anterior part	B	C	st	phr
T1p, superior temporal gyrus/posterior part	C	D	st	phr
T2a, middle temporal gyrus/anterior part	B	C	it	st
T2p, middle temporal gyrus/posterior part	C	D	it	st
TO2, middle temporal gyrus/temporooccipital part	D	F	it	st, ao
T3a, inferior temporal gyrus/anterior part	B	C	ot	it
T3p, inferior temporal gyrus/posterior part	C	D	ot	it
TO3, inferior temporal gyrus/temporooccipital part	D	F	ot	it
Parietal lobe				
POG, postcentral gyrus[b]	ce, *L*	poc, *ma*	phr	*ma*
SPL, superior parietal lobule	poc	F	ip	h.m.
SGa, anterior supramarginal gyrus	poc	D	phr, par	ip
SGp, posterior supramarginal gyrus	D	im, E	st	ip
AG, angular gyrus	im, E	ao, F	st, ao	ip
Occipital lobe				
OLs, superior occipital lateral gyri	F	G	lo	h.m.
OLi, inferior occipital lateral gyri	F	G	ot	lo
OP, occipital pole	G	h.m.	h.m.	h.m.
Medial Surface				
Frontal lobe				
FMC, frontomedial cortex	H, A	I	ol	sr
SMC, supplementary motor cortex.	J	K	ci	h.m.
Medial paralimbic cortices[c]				
SC, subcallosal cortex	I	l.t., s.p.	ol	ca
PAC, paracingulate cortex	H	Superior: J Inferior: I	ci	pa, sr
CGa, anterior cingulate gyrus	I	K	ca	ci
CGp, posterior cingulate gyrus	K	sp	ca, calc	ci, sp
Parietal and occipital lobes				
PCN, precuneus	ma	po	sp, calc	h.m.
CN, Cuneus	po	h.m.	calc	h.m.

plete the sulcal system with a set of coronal planes, defined by visible cerebral landmarks. The nomenclature devised for the parcellation system is mainly topographic and conservative for mnemonic convenience. The guidelines for the overall system are explicit so that it could be readily reproduced by other investigators. The boundaries for each region of interest are given in Table 2 and visualized in the cerebral maps of Figures 1 to 6. The approximate correspondences of the regions of interest to the systems oriented subdivisions and the Brodmann areas are reviewed in Table 3.

Validity of the Parcellation

The neural systems oriented model is ultimately based on cytoarchitectonic subdivisions, which are characterized by distinct corticocortical and thalamocortical connections. It derives from experimental studies of primate cortex and clinical evidence from the human brain (see reviews by Mountcastle, 1978; Mesulam, 1985; Pandya, & Yeterian, 1985). The model holds that human brain function reflects the operation of parallel distributed systems that are interconnected. Complex behavior is mapped

Table 2. *continued*

Parcellation unit	*Anterior border*	*Posterior border*	*Lateral border*	*Medial border*
Ventral Surface				
Frontal lobe				
FOC, frontoorbital cortex	A	s.p.	ahr	ol
Temporal and occipital lobes				
PHa, anterior parahippocampal gyrus	B	M	co	hi
PHp, posterior parahippocampal gyrus	M	N	co	hi
LG, lingual gyrus	N	G	co	calc
TFa, temporal fusiform gyrus/anterior part	B	C	ot	co
TFp, temporal fusiform gyrus/posterior part	C	D	ot	co
TOF, temporooccipital fusiform gyrus	D	F	ot	co
OF, occipital fusiform gyrus	F	G	ot	co
Intrasylvian Surface				
Frontoparietal operculum				
FO, frontal operculum	ahr	O	h.m.	cir
CO, central operculum	O	P	h.m.	cir
PO, parietal operculum	P	End of sy	h.m.	cir
Temporal operculum				
PP, planum polare	B	ftr	h.m.	cir
H1, Heschl's gyrus	ftr	he	h.m.	cir
PT, planum temporale	he	End of sy	h.m.	cir
INS, insula	cir	cir	cir	cir

[a]The regions of interest are specified in the first column, which also provides a key to their abbreviations. The cortical units are listed topographically in accordance with Figures 1 to 6. Abbreviations: Single capital letters indicate the limiting coronal planes (see Results and Figs. 1 to 6), small letters represent the limiting sulci (see Results and Figs. 1 to 6); h.m., hemispheric margin; l.t., lamina terminalis; s.p., substantia perforata anterior.
[b]Structures extending across the whole circumference of a given cerebral lobe.
[c]Structures extending across the lateral and medial brain surfaces. Their boundaries on the medial cerebral surface are listed in italics.
[d]Paralimbic cortices of the medial hemispheric surface that extend across the classical cerebral lobes (see also Tables 3, 4, and 5).

on these multifocal systems. Local networks subserving attention, memory, and language are "confined to single architectonic fields or to immediately contiguous areas" (Mesulam, 1990). These specific anatomical sites are of great interest as they relate to both the high-level parallel distributed functional architecture and the localized anatomically defined cytoarchitecture. The correlation between micro- and macroanatomical sites (Sanides, 1962) is the link that provides the theoretical basis for our approach.

The model is supported by functional imaging studies, which have shown that separate but interconnected cortical areas are activated by the appropriate specific behaviors (Roland, 1985; Petersen et al., 1988; Corbetta et al., 1991; Wise et al., 1991). These cortical areas of activation may correspond to cortical areas of microscopic specialization, though it is impossible to establish such correlations using in vivo imaging methods in humans. Interindividual anatomic variability is paralleled by physiological differences in the representation of sensorimotor (Penfield & Rasmussen, 1950; Woolsey, Erickson, & Gilson, 1979) and language functions (Ojemann, 1979, 1983).

Magnetic resonance imaging does not provide the means to differentiate the cortical architectonic fields directly. The coincidence of macroanatomic (sulcal, gyral) and microanatomic (cytoarchitectonic) borders (Sanides, 1962) is the critical assumption for imaging studies on structure–function relationships. It has abundant precedent in contemporary approaches to defining anatomical correlates of higher brain functions (Mesulam, 1985; Damasio & Damasio, 1989; Greitz et al., 1991).

Interindividual and interhemispheric variations in the topography and size of architectonic fields (von Economo & Horn, 1930; Filimonoff, 1932; Strasburger, 1938; Schulze, 1960; Sarkisov, 1966; Stensaas, Eddington, & Dobelle, 1974; Galaburda et al., 1978; Rademacher, Caviness, Steinmetz, & Galaburda, 1992) represent the limitations of this approach. A strict covariance between cytoarchitectonic variability and individual convolutional pattern cannot be assumed. First, cytoarchitectonic differences can be greater (area tpt vs. planum temporale) or smaller (primary auditory cortex vs. transverse Heschl gyri) than associated differences in the convolutional pattern (Galaburda et al., 1978; Galaburda & Sanides, 1980). Second, the distribution of individual architectonic fields varies within specific cortical regions. For example, area PG can represent between 16 and 85% of the cortical volume of the angular gyrus (Eidelberg & Galaburda, 1984). Third, divergent architectonic asymmetries (area PG vs. area PEG) exist within homogeneous

Table 3. Corresponding (Cortical) Parcellation Units, Brodmann Areas, and Functional Regions.[a]

Parcellation unit	*Brodmann area*	*Functional region*
Frontal lobe		
FP, frontal pole	10, 11	HFA
F1, superior frontal gyrus	6, 8, 9	PMC, HFA
F2, middle frontal gyrus	6, 8, 9, 46	FEF, PMC, HFA
F3t, inferior frontal gyrus	45	HFA
F3o, inferior frontal gyrus	44	MA
PRG, precentral gyrus	6, 4	M1
SMC, supplementary motor cortex	Medial 6	SMA
FMC, frontomedial cortex	11, 12	HFA
FOC, frontoorbital cortex	47	HFA
FO, frontal operculum	45, 44	HFA, MA
CO, central operculum	43	HSA
Temporal lobe		
TP, temporal pole	38	POA
T1a, superior temporal gyrus	Anterior 22	AA2, AA3
T1p, superior temporal gyrus	Posterior 22	AA1
T2a, middle temporal gyrus	Anterior 21	VA
T2p, middle temporal gyrus	Posterior 22	VA
TO2, middle temporal gyrus	37	VA
T3a, inferior temporal gyrus	Anterior 20	VA
T3p, inferior temporal gyrus	Posterior 20	VA
TO3, inferior temporal gyrus	37	VA
TFa, temporal fusiform gyrus	36, 20	PHA, VA
TFp, temporal fusiform gyrus	36, 20	PHA, VA
TOF, temporooccipital fusiform gyrus	37	VA, PHA
PP, planum polare	Anterior 22	POA
INS, insula	13, 14, 15, 16	POA
H1, Heschl's gyrus	41	A1
PT, planum temporale	42, 40, Posterior 22	AA1
Parietal lobe		
POG, postcentral gyrus	3a, 3b, 1, 2, (5)	S1, SA
SPL, superior parietal lobule	5, 7	SA, HPA
SGa, supramarginal gyrus	Anterior 40	HPA
SGp, supramarginal gyrus	Posterior 40	HPA
AG, angular gyrus	39	HPA
PCN, precuneus	Medial 7	SSA, SA, HPA
PO, parietal operculum	40	SA, AA, HPA
Occipital lobe		
OLs, occipital lateral gyri	18, 19	VA
OLi, occipital lateral gyri	18, 19	V5
OP, occipital pole	17, 18	V1, V2
CN, cuneus	17, 18, 19	V1, V2, V3
LG, lingual gyrus	17, 18	V1, V2, V3
OF, occipital fusiform gyrus	19	V4
Medial paralimbic cortices[b]		
SC, subcallosal cortex	25, Posterior 32	PHA
PAC, paracingulate cortex	32	PHA
CGa, cingulate gyrus	33, 24	PHA
CGp, cingulate gyrus (includes retrosplenial cortex)	23, 31, 26, 29, 30	PHA
PHa, parahippocampal gyrus	28, 34	PHA
PHp, parahippocampal gyrus	27, 35	PHA

[a]The specific cortical structures (first column) are abbreviated (see Table 2 for key to abbreviations). The comparison is meant as a scheme for orientation. The parcellation units are ordered according to cerebral lobes (from lateral to medial, ventral, and opercular surfaces). Abbreviations (functional regions): AI, primary auditory cortex; VI, primary visual cortex; SI, primary somatosensory cortex; MI, primary motor cortex; AA, auditory association cortex (specified as AA1, AA2, AA3); VA, visual association cortex (specified as V2, V3, V4, V5); SA, somatosensory association cortex; SSA, supplementary somatosensory area; MA, motor association cortex (specified as PMC, premotor cortex; SMA, supplementary motor area; FEF, frontal eye field); HFA, heteromodal frontal association cortex; HSA, heteromodal subcentral association cortex; HPA, heteromodal parietal association cortex; POA, paralimbic olfactocentric association cortex; PHA, paralimbic hippocampocentric association cortex.
[b]Because of their concentric extent across the classical lobes, the paralimbic structures of the medial brain surface are listed separately.

structures (angular gyrus) and cannot be inferred from the analysis of the macroanatomic pattern.

Morphometry

The present parcellation system provides specific cortical compartments for the whole cerebral hemisphere. To our knowledge, the acquisition of regional volumes for the whole cerebral cortex at this spatial resolution has not been achieved in any prior study. The present approach provides for anatomical analyses not achievable via postmortem study. The introduction of proportional values in addition to absolute figures is of importance as it permits interindividual comparisons independent of variations in absolute brain size (Table 4). It also enables us to compare some of our volumetric data with the area measurements (Table 5) of Jouandet et al. (1989). Although the small number does not support specific conclusions, some general patterns are of interest. Our values for the relative representation of the frontal, temporal, parietal, and occipital lobes agree well with previously published in vivo (Jouandet et al., 1989) and postmortem (Zilles, 1990) data. Even at this gross level of analysis the differences between the identical twins studied by Jouandet et al. are frequently greater than the variation between one of them and our normal control. The same is true for the comparison of cortical structures at the gyral level (Table 5). It is of interest to note that in both studies approximately two-thirds of the cortical parcellation units were asymmetric (interhemispheric difference larger than 10%). Our separate measurements of three functionally important intrasulcal cortices (intrasylvian, intraparietal, and intracalcarine cortices) underline the dimensions of cortical folding. Together, sylvian fissure and intraparietal sulcus contain approximately 10% of the total cortical volume.

At this time it is premature to evaluate diverging results. The range of interindividual and interhemispheric variability in the human brain is not known. On the other hand, the techniques for data acquisition differ considerably. There are confounding factors. The regions of interest were not defined explicitly in the publication of Jouandet et al. (1989). That study provided measures of cortical area while the present provides measures of cortical volume. Finally, the geometric transformations involved in the analysis of Jouandet et al. may in themselves have been a source of variation.

The functional relevance of quantitative macroanatomic data is a complex issue. Based on animal models (Goldman-Rakic & Rakic, 1984; Galaburda, Aboitiz, Rosen, & Sherman, 1985; Rakic, 1988; Rosen, Sherman, & Galaburda, 1989), it is assumed that morphological differences reflect differences in the number of neuronal populations and interhemispheric connections and therefore relate to the functional capacity of a given structure. A discussion of this assumption is beyond the scope of our study. For example, planum temporale size asymmetries are supposed to underlie functional language lateralization, but the distribution of anatomical asymmetries (leftward asymmetry in 73.5% of 520 adult brains; Steinmetz et al., 1990c) appears to be too low compared with the functional data (leftward asymmetry in 95% of the population). Much depends on the definition of the anatomical boundaries of the cortical regions. For example, a significant correlation has been shown between left-handers with familial sinistrality and symmetric plana only when the terminal ascending portion of the planum temporale was excluded from the measures (Steinmetz, Volkmann, Jäncke, & Freund, 1991). In addition, the definition of functional language lateralization varies according to the method that is applied. Intracarotid amobarbital injection specifies functional lateralization of speech production, but does not provide evidence for the laterality of comprehension of word meaning (Hart, Lesser, Fischer, Schwerdt, Bryan, and Gordon, 1991). Finally, functional competence depends on successful synaptogenesis, which has been shown to increase for an extended period after birth (Huttenlocher, 1979; Rakic, Bourgeois, Eckenhoff, Zecevic, & Goldman-Rakic, 1986), parallel to the critical postnatal period for the development of speech lateralization (Marcotte & Morere, 1990). These important events for the functional mapping of a given capacity occur well after the formation of the typical anatomical asymmetries has been completed (Wada, Clarke, & Hamm, 1975). They are sensitive to modulations imposed by nongenetic extrinsic mechanisms.

Functional and Anatomical Zones

The present approach represents a substantial advance in defining and quantifying the gross anatomy of human cerebral cortex using MR. While the relationship between functional systems and anatomical parcellations is complex, the present approach provides a means for investigating structure–function correlations via the detailed analysis of size asymmetries in normal subjects and lesion localization in neurological patients.

Discrepancies between published cytoarchitectonic maps of the human brain (Brodmann, 1909; von Economo and Koskinas, 1925; Sanides, 1962; Braak, 1980) further confound correlations between microscopic and macroscopic definitions of cortex. In general, we will refer to Brodmann's system. In addition, specific brain regions elaborated by other investigators will be quoted. An extensive comparison and critique of the various maps and nomenclatures has been given elsewhere (Zilles, 1990). The description of the functional systems has to be schematic. The subsequent discussion follows the hierarchy of the functional systems, whereas Table 3 provides an overall comparison that is structured in relation to the anatomical compartments.

Table 4. Volume Measurements (cm^3) and Proportional Values (%) for (Cortical) Parcellation Units of Left and Right Hemispheres in One Human Brain.[a]

Parcellation unit	*Left volume (cm^3)*	*Left volume (%)*	*Right volume (cm^3)*	*Right volume (%)*
Frontal lobe				
FP, frontal pole	26.72	7.62	27.96	7.99
F1, superior frontal gyrus	18.68	5.33	20.11	5.75
F2, middle frontal gyrus	15.78	4.50	13.14	3.76
F3t, inferior frontal gyrus	2.26	0.64	3.31	0.95
F3o, inferior frontal gyrus	3.24	0.92	2.42	0.69
PRG, precentral gyrus	16.80	4.79	18.20	5.20
SMC, supplementary motor cortex	6.13	1.75	5.01	1.43
FMC, frontomedial cortex	3.86	1.10	2.56	0.73
FOC, frontoorbital cortex	10.08	2.87	12.02	3.44
FO, frontal operculum	3.63	1.04	3.68	1.05
CO, central operculum	5.04	1.44	6.15	1.76
Total frontal lobe	*112.22*	*32.00*	*114.56*	*32.74*
Temporal lobe				
TP, temporal pole	12.01	3.42	9.76	2.79
T1a, superior temporal gyrus	1.41	0.40	1.88	0.54
T1p, superior temporal gyrus	3.91	1.11	6.03	1.72
T2a, middle temporal gyrus	2.81	0.80	2.50	0.71
T2p, middle temporal gyrus	6.36	1.81	7.79	2.23
TO2, middle temporal gyrus	10.83	3.09	10.45	2.99
T3a, inferior temporal gyrus	3.39	0.97	2.39	0.68
T3p, inferior temporal gyrus	9.64	2.75	7.28	2.08
TO3, inferior temporal gyrus	7.25	2.07	8.46	2.42
TFa, fusiform gyrus	1.56	0.44	1.62	0.46
TFp, fusiform gyrus	5.99	1.71	4.81	1.37
TOF, fusiform gyrus	9.40	2.68	8.43	2.41
PP, planum polare	1.60	0.46	1.88	0.54
INS, insula	8.48	2.42	7.50	2.14
H1, Heschl's gyrus	1.35	0.38	1.54	0.44
PT, planum temporale	4.62	1.32	6.03	1.72
Total temporal lobe	*90.61*	*25.84*	*88.35*	*25.25*

Primary Cortices

The primary cortices deal with the analysis of the primary signal in one modality.

Primary Auditory Cortex. The primary auditory cortex (A1) or Brodmann area 41 is located on the first transverse gyrus of Heschl (Pfeifer, 1920, 1936). It is surrounded by belt areas (Galaburda and Sanides, 1980) that lie on the adjacent temporal surface. The extent of the belt areas is unclear, with the differences between the studies being greater than the assumed interindividual anatomical variability (Zilles, 1990). The frequent side differences in the number of transverse gyri (up to 50% rightward asymmetry; von Economo & Horn, 1930) are not related to asymmetries of Brodmann area 41. When Heschl's gyrus is subdivided by an intermediate sulcus into an anterior and posterior portion, area 41 is usually restricted to the former (Rademacher et al., 1992).

Primary Visual Cortex. The human primary visual cortex (V1), the physiological definition of which correlates with Brodmann's delineation of area 17, lies within and around the calcarine sulcus. At the occipital pole (coronal plane G) it may extend onto the lateral brain surface, but this is not the rule (Stensaas et al., 1974). The parietooccipital sulcus is the reliable anterior border for the maximal surface extent of the supracalcarine portion of area 17. Independent of the hemisphere, 92% (mean value) of the total amount of area 17 lies posterior to the intersection of the parietooccipital and calcarine sulci (cuneal point; Rademacher et al., 1992). On the average the amount of intracalcarine area 17 represents 62% of total striate cortex. The volume of intracalcarine cortex (posterior segment) may serve as an indicator for the overall size of area 17. Interhemispheric asymmetries are small compared to interindividual variations, such that most brains are symmetric with respect to area 17.

Primary Somatosensory Cortex. In nonhuman primates Brodmann area 3b corresponds to physiologically defined primary somatosensory cortex (S1; Kaas & Pons, 1988). In the human brain area 3b lies on the caudal lip of the central sulcus and in general does not reach the

Table 4. *continued*

Parcellation unit	*Left volume (cm^3)*	*Left volume (%)*	*Right volume (cm^3)*	*Right volume (%)*
rietal lobe				
POG, postcentral gyrus	17.66	5.04	15.24	4.36
SPL, superior parietal lobule	13.13	3.74	15.92	4.55
SGa, supramarginal gyrus	8.76	2.50	5.22	1.49
SGp, supramarginal gyrus	4.47	1.27	10.92	3.12
AG, angular gyrus	13.17	3.76	11.74	3.36
PCN, precuneus	11.49	3.28	10.78	3.08
PO, parietal operculum	5.56	1.59	4.65	1.33
Total parietal lobe	*74.24*	*21.17*	*74.47*	*21.28*
Occipital lobe				
OLs, occipital lateral gyri	8.45	2.41	7.83	2.24
OLi, occipital lateral gyri	4.16	1.19	4.11	1.17
OP, occipital pole	6.78	1.93	7.60	2.17
CN, cuneus	8.99	2.56	9.03	2.58
LG, lingual gyrus	11.67	3.33	12.26	3.50
OF, fusiform gyrus	1.79	0.51	1.59	0.45
Total occipital lobe	*41.84*	*11.93*	*42.42*	*12.12*
Medial paralimbic cortices[b]				
SC, subcallosal cortex	1.97	0.56	2.29	0.65
PAC, paracingulate cortex	8.74	2.49	8.34	2.38
CGa, cingulate gyrus	7.11	2.03	6.04	1.73
CGp, cingulate gyrus	7.28	2.08	7.23	2.07
PHa, parahippocampal gyrus	3.26	0.93	3.15	0.90
PHp, parahippocampal gyrus	1.48	0.42	1.22	0.35
H, hippocampus	1.94	0.55	1.83	0.52
Total medial paralimbic cortices	*31.78*	*9.06*	*30.10*	*8.60*
Total cerebral cortex	**350.69**		**349.90**	
ip, intraparietal sulcus[c]	11.00	3.14	11.79	3.37
sy, sylvian fissure[c]	25.08	7.15	26.85	7.67
calc, calcarine sulcus[c]	3.03	0.86	3.10	0.89

[a]The parcellation units are ordered according to cerebral lobes (from lateral to medial, ventral, and opercular surfaces). The abbreviations (see Table 2 for key to abbreviations) specify each region of interest.
[b]For convenience the hippocampus proper is listed together with the medial paralimbic cortices.
[c]Three cerebral sulci (sylvian, intraparietal, calcarine) and the planum temporale horizontalis were measured independently.

medial brain surface (Braak,1980). Electrophysiological recordings in human anterior parietal cortex have also shown distinct functional representations for Brodmann areas 3a, 3b, 1, and 2 (PA, PB, PC, and PD; von Economo & Koskinas, 1925; review by Kaas, 1990). Individual differences in the localization of the foot area relative to the hemispheric margin have been described (Woolsey, Erickson, & Gilson, 1979). Medially, coronal plane L is the anterior border of the parietal lobe. The marginal sulcus represents the boundary between the anterior (postcentral) and posterior parietal architectonic fields (Sanides, 1962).

Primary Motor Cortex. The precise extent of the primary motor cortex (M1) is still debated (Zilles, 1990). Brodmann area 4 covers the middle third of the paracentral lobule, the free surface of the upper precentral gyrus, and the anterior bank of the central sulcus (Brodmann, 1909). Its extent on the exposed cerebral surface is exaggerated on the classical Brodmann map as shown with both pigmentarchitectonic (Braak, 1980) and cytoarchitectonic (Rademacher et al., 1992) techniques. At the level of the inferior frontal sulcus Brodmann area 4 is located exclusively within the depth of the central sulcus. Posterior area 6 on the precentral gyrus appears to be also part of M1 (Wise and Strick, 1984).

Unimodal Association Cortices

The unimodal association areas are involved in complex modality specific analyses. With increasing distance from the primary areas, there is an increase in multimodal integration.

Auditory Association Cortex. The auditory association cortices (AA), which can be subdivided (coronal plane C) into anterior (AA2 and AA3) and posterior (AA1) parts (Pandya & Yeterian, 1985), are located on the supratem-

Table 5. Comparison between Proportional Values for Selected (Cortical) Parcellation Units from the Present Study (Control) and from the Study (Twin A and B) of Jouandet et al. (1989)[a]

Parcellation unit	*Left volume (%) Control*	*Left area (%) Twin A*	*Left area (%) Twin B*	*Right volume (%) Control*	*Right area (%) Twin A*	*Right area (%) Twin B*
Frontal lobe						
Inferior frontal gyrus (F3t)	0.64	3.55	2.38	0.95	3.86	2.81
Inferior frontal gyrus (F3o)	0.92	2.11	2.04	0.69	2.26	1.87
Precentral gyrus (PRG)	4.79	4.47	3.62	5.20	4.53	3.85
Temporal lobe						
Superior temporal gyrus (PP, H1, PT, T1a, T1p)	3.67	4.21	5.09	4.96	5.73	5.72
Middle temporal gyrus (T2a, T2p, TO2)	5.70	5.79	4.52	5.93	5.46	4.99
Inferior temporal gyrus (T3a, T3p, TO3)	5.79	6.97	3.62	5.18	3.86	4.78
Insula (INS)	2.42	3.03	2.71	2.14	2.13	2.70
Heschl's gyrus (H1)	0.38	0.26	0.90	0.44	0.93	0.73
Planum temporale (PT)	1.32	0.39	0.34	1.72	0.53	0.31
Parietal lobe						
Postcentral gyrus (POG)	5.04	5.92	5.32	4.36	9.32	6.13
Superior parietal lobule (SPL, PCN)	7.02	8.82	7.81	7.63	7.72	8.42
Supramarginal gyrus (SGa, SGp)	3.77	2.63	4.41	4.61	4.39	3.12
Angular gyrus (AG)	3.76	2.24	1.58	3.36	1.73	1.98
Medial paralimbic cortices						
Cingulate gyrus (CGa, CGp)	4.11	4.21	2.94	3.80	2.93	3.33

[a]Abbreviations (see Table 2 for key to abbreviations) in parentheses represent the parcellation units of the present study, which have been combined for this purpose. The values are derived from volumetric (Control) and area (Twins) measurements.

poral plane and on the lateral surface of the first temporal gyrus. The planum temporale and the posterior part of the first temporal gyrus belong to Wernicke's language region (Bogen & Bogen, 1976) and relate to the temporal magnopyramidal area (Braak, 1980) and area tpt (Galaburda et al., 1978). In the depth of the sylvian fossa the secondary auditory cortex (A2) and area tpt reach onto the parietal operculum. Area tpt asymmetries correlate with the side differences of the planum temporale, and with asymmetries of parietal area PG (Eidelberg & Galaburda, 1984). They are paralleled by asymmetries of Brodmann area 44, which is part of Broca's region (Galaburda, 1980). These associations of gyral and cytoarchitectonic asymmetries may reflect in part intricate structural and functional connections. Asymmetries of the planum temporale correlate with developmental syndromes (Galaburda et al., 1985; Geschwind & Galaburda, 1985) and handedness (Steinmetz et al., 1991). Verbal auditory stimulation results in a left-lateralized increase in glucose metabolism (Mazziotta, Phelps, Carson, & Kuhl, 1982) and cerebral blood flow (Petersen, Fox, Posner, Mintun, & Raichle, 1988) in the planum temporale, which represents an essential component of the distributed cortical network of word comprehension (Mesulam, 1990; Wise et al., 1991).

Visual Association Cortex. The topography of primate visual association areas [VA; (Zeki, 1978; Van Essen, 1985)] can be characterized in the human brain by the distribution of callosal afferents (Clarke & Miklossy, 1990). The ventral parts of V2 (visual area II) and V3 (ventral posterior visual area VP) lie on the lingual gyrus. V4 lies on the posterior fusiform gyrus [area OA; (von Economo & Koskinas, 1925)]. Dorsal V2 and V3 lie on the cuneus and V5 (middle temporal area MT) lies on the lateral occipital gyri near the occipitotemporal junction. V2 and V3 are parts of Brodmann area 18, and V4 and V5 are parts of Brodmann area 19.

The superior visual association cortices have been related to spatial analysis, and the inferior cortices to pattern recognition and color reception (Mishkin, Ungerleider, & Macko, 1983; Damasio, 1985). For example, the posterior part of the human fusiform gyrus participates in color vision (review by Zeki, 1990). The anatomical dichotomy of cuneal and lingual/fusiform compartments may relate to two distinct and parallel structural–functional systems, the magnocellular and the parvocellular (Livingstone & Hubel, 1988). On the lateral hemisphere, the superior occipital gyri and the upper banks of the anterior occipital sulcus play a role in the perception of visual motion (Zihl, von Cramon, Mai, & Schmid, 1991). The intraparietal sulcus contains Brodmann area 2 rostrally, and Brodmann area 19 caudally. The integration of visual and somatosensory information may be an associated heteromodal function (Seltzer & Pandya, 1980). The inferior parts of lateral occipital cortex belong to a network that is supposed to generate visual word form without participation of the phono-

ɔgical coding regions of temporoparietal cortex (Peter-
ɔn et al., 1988; Petersen, Fox, Snyder, & Raichle, 1990).
. "basal temporal language area" has been localized on
nterior part of the fusiform gyrus in the dominant
emisphere (Lüders et al., 1986, 1991).

Analogous to the auditory association areas, the visual
ssociation areas on the lateral and ventral surfaces of
ıe temporal lobe (Brodmann areas 20 and 21) can be
ubdivided in coronal plane C into anterior and posterior
egments (Braak, 1980; Pandya & Yeterian, 1985). The
audally adjacent temporooccipital cortex (Brodmann
rea 37) lying between coronal planes D and F also
xtends from the lateral to the ventral brain surface. It
ıcludes the middle and inferior temporal gyri as well
s the fusiform gyrus.

ɔomatosensory Association Cortex. The somatosensory
ıssociation cortex (SA) on the superior parietal lobule
ɔnsists of Brodmann area 5 and the lateral part of Brod-
nann area 7 (PA2, PE; von Economo & Koskinas, 1925;
review by Kaas, 1990). It belongs to a network for the
listribution of directed attention in extrapersonal space
Mesulam, 1990) and seems to be asymmetrically orga-
ıized. The right hemisphere attends to both sides, while
he left hemisphere is restricted to contralateral space. A
ɔossible correlation between left-lateralized language
unctions and right-lateralized attentional mechanisms
remains to be shown both anatomically and functionally.

The supplementary sensory area (SSA) is supposed to
ie on the precuneus (medial Brodmann area 7), above
he subparietal sulcus. Secondary somatosensory cortex
(S2) lies on the parietal operculum in the depth of the
ylvian fissure (Penfield & Rasmussen, 1950; Woolsey
et al., 1979).

Motor Association Cortex. The unimodal motor asso-
ciation cortex (MA) contains the premotor cortex (PMC),
the supplementary motor area (SMA), the posterior fron-
tal eye field (FEF), and Brodmann area 44. Dorsolaterally,
the premotor cortex (anterior part of Brodmann area 6)
covers the posterior part of the superior frontal gyrus,
just in front of the primary motor area. The supplemen-
tary motor area (medial Brodmann area 6) is located on
the medial surface of the superior frontal gyrus, rostral
to the precentral leg area [coronal plane K; (Penfield &
Rasmussen, 1950; Woolsey et al., 1979)]. As a "supramotor
area" it is involved in the programming, initiation, and
execution of sequential movements (Roland, 1984, 1985).
The supplementary motor cortex and the premotor cor-
tex are included in Braaks' superofrontal magnopyra-
midal region (Braak, 1980). The frontal eye field
(Brodmann area 8) extends from the middle frontal gy-
rus onto the precentral gyrus (Woolsey et al., 1979; Ro-
ıd, 1984). Brodmann area 44, lying on the pars
ɔpercularis of the inferior frontal gyrus, is part of the
speech region (Broca's area).

Heteromodal Association Cortices

The heteromodal association areas are crucial for inter-
modal integration and sensory-limbic transformations
(Mesulam, 1985), with the former being more pro-
nounced in the temporoparietal zone and the latter in
the prefrontal region. These zones show the highest
degree of gyrification (i.e. folding; Zilles, Armstrong,
Schleicher, & Kretschmann, 1988).

Prefrontal Association Cortex. The prefrontal associa-
tion cortex is related to complex aspects of behavior and
personality. Distinct afferents from unimodal association
areas to separate prefrontal areas indicate specific con-
tributions to defined networks (Mesulam, 1985). Sanides
(1962) provides the most extensive architectonic analysis
of the frontal lobe. In a fashion analogous to the func-
tional subdivisions of the frontal cortex (Roland, 1984;
Roland, 1985), the parcellation of Sanides respects the
horizontal orientation of the frontal gyri on the lateral
cerebral surface. Because distinct surface structure land-
marks (intermediate frontal sulcus; Ono et al., 1990)
were not appreciated, we could not subdivide the middle
frontal gyrus into superior (inferior Brodmann area 8)
and inferior (Brodmann areas 46 and 9) portions.

Our approach captures the subdivision of inferior
frontal cortex into three (orbital, triangular, and oper-
cular) parts defined by Eberstaller (1890) and Brodmann
(1909). The speech region is located on the pars oper-
cularis (Brodmann area 44) and pars triangularis (Brod-
mann area 45) of the inferior frontal gyrus (Mohr et al.,
1978). The anterior ascending ramus of the sylvian fissure
marks their common boundary. In 64% of the right hemi-
spheres and 72% of the left hemispheres (Ono et al.,
1990) the course of the diagonal sulcus represents the
border (Galaburda, 1980). Both areas extend partly onto
the frontal operculum. The adjacent pars orbitalis (Brod-
mann area 47), which seems to participate in processing
for semantic association (Petersen et al., 1988), and the
rostral insula are functionally related to this region (Mohr
et al., 1978) and are architectonically similar (Sanides,
1962). As with the inferior parietal lobule, the range of
architectonic variations (Riegele, 1931; Kreht, 1936) cor-
relates with the individual gyral patterns. The functional
asymmetry of speech is related to only small anatomical
asymmetries (Witelson & Kigar, 1988; Albanese, Merlo,
Albanese, & Gomez, 1989), which are further obscured
by varying definitions of the speech region between dif-
ferent observers.

Our parcellation of the frontoorbital and frontomedial
surfaces is derived from Sanides' work (Sanides 1962).
The frontomedial cortex covers the medial orbital gyrus
and the straight gyrus. The medial orbital sulcus is the
constant lateral field boundary of Brodmann area 11
(Sanides, 1962). Because of its constancy (100%; Ono
et al., 1990), the olfactory sulcus is a more reliable land-
mark. The frontal pole, defined posteriorly by coronal

planes A (lateral and ventral surfaces) and H (medial surface), relates dorsally to Brodmann area 10 and ventrally to Brodmann area 11. The transverse orbital sulcus is an important additional landmark, subdividing the orbital brain surface into anterior and posterior parts (Sanides, 1962). It coincides approximately with coronal plane A.

Subcentral Association Cortex. The intrasylvian central operculum is continuous with the precentral and postcentral gyri (Fig. 5, between coronal planes O and P). Architectonically it represents a fusion of precentral and anterior parietal features (Braak, 1980). It relates both to motor and sensory functions.

Temporoparietal Association Cortex. The cytoarchitectonic variability of the temporoparietal association cortex (Brodmann areas 39 and 40) is related to the individual gyral patterns (Schulze, 1960). For the inferior parietal lobule (areas PF and PG; von Economo & Koskinas, 1925), the precentral, intraparietal, and anterior occipital sulci represent approximate sulcal boundaries. The intermediate sulcus of Jensen (coronal plane E) marks the posterior border of transition zone PFG on the supramarginal gyrus, and the angular sulcus is surrounded by area PG (Eidelberg & Galaburda, 1984). In agreement with earlier studies (Critchley, 1953) the dorsal end of the parietooccipital sulcus at the hemispheric margin is taken to represent the "nodal point" for the definition of the caudal border of the parietal cortices (coronal plane F). Cytoarchitectonically, the caudal limits of the inferior and superior parietal lobules consist of transition zones OPE, OPG, and OPH (Eidelberg & Galaburda, 1984).

Mesulam (1990) indicates that one functional specialization of parietal area PG is the processing for directed attention. The right hemisphere is dominant for this function. Cytoarchitectonic area PF and the ventral part of area PG belong to the network for language. In right-handers the left hemisphere is dominant for this function. Direct correlations with the leftward asymmetry of area PG and the rightward asymmetry of area PEG (Eidelberg & Galaburda, 1984) are not established. The same is true for lateralized differences in the opercular part of the supramarginal gyrus (Steinmetz et al., 1990a).

Paralimbic Association Cortices

The paralimbic association cortex can be subdivided into two subregions. The olfactocentric formation (POA) consists of the temporal pole, insula, and caudal frontoorbital cortex. The hippocampocentric group (PHA) includes the parahippocampus, cingulate gyrus, retrosplenial cortex, paracingulate, and subcallosal regions. The whole paralimbic belt is involved in components of memory function (Mesulam, 1985).

Olfactocentric Paralimbic Association Cortex. The insula is subdivided into an anterior and posterior portion by its central sulcus (Retzius, 1896). Its organization is concentric, with an anteroventral allocortical core (Ia-p), an intermediate belt (Idg), and a dorsal isocortical area [Ig; (Brockhaus, 1940; Mesulam & Mufson, 1985)]. Ia-p participates in the control of autonomic function, alimentary behavior, and affect. Anatomically and functionally it is related to the temporal pole and the caudal part of the frontoorbital cortices (caudal Brodmann areas 11 and 12). Ig is involved in auditory, somatosensory and motor functions (Mesulam & Mufson, 1985).

Hippocampocentric Paralimbic Association Cortex. The rostral parahippocampal gyrus contains the subicular complex, which has limbic components, and the entorhinal cortex (Brodmann areas 28 and 34) (Braak, 1980). Along the collateral sulcus it is bordered laterally by the perirhinal cortex (Brodmann areas 35 and 36). The entorhinal cortex extends approximately from the frontotemporal junction (coronal plane B) to the lateral geniculate nucleus (coronal plane M) (Amaral & Insausti, 1990). Caudally it is continuous with cytoarchitectonic areas TH and TF (von Economo & Koskinas, 1925). Primate posterior parahippocampus, extending posteriorly to the level of the anterior end of the calcarine sulcus (coronal plane N), represents a sensory convergence zone (Van Hoesen, 1982).

At the level of the cingulate isthmus, the concentric retrosplenial cortex (Brodmann areas 26, 29, and 30) lies adjacent to the splenium of the corpus callosum. The cingulate gyrus is subdivided into an agranular anterior part (Brodmann areas 33 and 24) and a granular posterior part (Brodmann areas 23 and 31). The border lies approximately at the level of the dorsomedial precentral sulcus (coronal plane K) (Sanides, 1962). The connections of the anterior portion and recent activation studies with positron emission tomography (Petersen et al., 1988) indicate a role in attentional mechanisms.

The paracingulate region (Brodmann area 32) lies parallel to the cingulate gyrus, above the superior rostral sulcus. It is related to the double parallel type of the cingulate sulcus (Ono et al., 1990), which is present in 24% of the brains. Being located between the superior frontal gyrus and the anterior cingulate gyrus, area 32 covers approximately the middle third of the medial cerebral surface, which is our criterion when there is no paracingulate sulcus. According to classic maps (Brodmann, 1909; von Economo & Koskinas, 1925) the paracingulate region extends posteriorly to the level of the anterior commissure (coronal plane J) (Talairach et al., 1967). This boundary may be located more caudally at the level of the dorsal precentral sulcus (Sanides, 1962). The subcallosal (parolfactory) region, classically defined by the genu of the corpus callosum (coronal plane I), contains Brodmann area 25. It also includes portions of the cingulate gyrus, paracingulate area 32, and fronto-

medial cortex (posterior Brodmann areas 11 and 12). It extends onto the straight gyrus (von Economo & Koskinas, 1925).

Limbic System

Our parcellation system is devised for the isocortical and mesocortical areas of the human brain. We refer here only briefly to the limbic system, which may be analyzed in comparable fashion with MRI (Naidich et al., 1987). The hippocampal formation (defined as the fimbria, dentate gyrus, hippocampus proper, and subiculum) can be reliably identified by its ventromedial location in the temporal lobe, just posterior to the amygdala and above the hippocampal fissure. Its characteristic shape can be outlined throughout most of its rostrocaudal extent. As an anatomic convention, the coronal plane containing the posterior commissure may be defined as its caudal border. The amygdala appears as an ovoid structure, which is directly continuous with the uncus of the parahippocampal gyrus.

FUTURE APPLICATIONS

On the basis of the conceptual framework provided by Mesulam (Mesulam, 1985, 1990), we have presented an approach to the in vivo anatomical analysis of human cerebral cortex, which provides both a revision of classic systems models and computational methodology for its implementation in MR images. Our method provides the anatomical detail needed for structure–function correlations. We view this system as a tool for correlative studies of interhemispheric and interindividual differences at the neuroanatomical, behavioral, and neurocomputational level. It is ideally suited for the three-dimensional matching of individual anatomic and functional data (Pelizzari, Chen, Spelbring, Weichselbaum, & Chen, 1989; Pietrzyk, Herholz, & Heiss, 1990), and it may have special value when applied to future functional MR mapping studies (Belliveau et al., 1992).

Potential applications of our method to the study of brain–behavior relationships include morphometric studies of normal individuals, quantitative lesion localization studies in neurological patients, and anatomical mapping of functional images obtained via activation studies. In either case the cerebral lesions or foci will very likely span parcellation boundaries or spread only subtotally through a set of regions of interest. The fineness of grain of localization can be readily advanced simply by subdividing the cortical regions of interest by individual grid overlays. This strategy could flexibly provide multiple parameters including a metric of localization and proportionality. Ultimately, as analyses accumulate, subcomponents of information processing algorithms could be mapped as an overlay onto the parcellation system.

METHODS

The method of cerebral localization, parcellation, and morphometry was applied to the 3D-FLASH MR scan of a normal 26-year-old male volunteer. The MR scan was obtained on a 1.0 Tesla Siemens Magnetom MR System utilizing an optimized 3D-FLASH sequence. The T1-weighted gradient echo pulse sequence had the following technical parameters: 40 msec repetition time, 15 msec echo time, 50 degrees flip angle, 2 averages, and a 256 × 256 image matrix. The MR volume data were partitioned into 63 contiguous coronal slices of 3.1 mm thickness and an in plane resolution of 1.17 mm.

Image Data Analysis

The image data were transferred to a Sun Microsystems 4/330 workstation for morphometric analysis. For comparisons of the two sides of the brain, it is important to avoid brain rotation. We applied a retrospective positional normalization technique to the volumetric MRI data. Initially the brain is placed in a cartesian coordinate system wherein the anterior–posterior commissure line (AC–PC line) defines the Y axis. The Z plane is constructed from the Y axis in the interhemispheric fissure, while the coronal plane is orthogonal to Y axis and Z plane (Talairach et al., 1967). To achieve the complete parcellation of the human brain, our method relies on the identification of brain sulci in the three standard imaging planes (coronal, transaxial, sagittal). We reconstructed a "true" coronal image data set, as well as transaxial and sagittal planes by reslicing the image data in the X, Y, or Z planes as determined by the cartesian coordinate system. Subsequently, computerized intensity contour and differential contour algorithms (Kennedy, Filipek, & Caviness, 1989) were used to obtain continuous outlines of the cerebral surface and of the gray and white matter border (Filipek et al., 1989).

Within the cartesian coordinate system a given spatial location in any of the image data sets can be related to a location in any of the other images, by the application of a coordinate transformation ("point-to-point" transfer). We applied this transformation to both, individual points and line segments, which enabled us to project sulcal outlines between the image data sets (Figs. 7, 8, and 9). Within the stereotaxic system, any rotation of the MR-data set could be reliably performed. In the optimum plane of view the course of a sulcus is digitized with a hand-controlled "mouse." The trace will be represented as a point in any slice of the coronal series in which intersection occurs. Where a point is encountered the cortical ribbon is divided with the mouse-driven cursor. When a sulcus is localized the boundary is marked in the depth of the sulcus.

The identified sulci are listed with the key to abbreviations in Table 1 (see also Figs. 1 to 6). For morphometry, the regions of interest were defined by their limiting

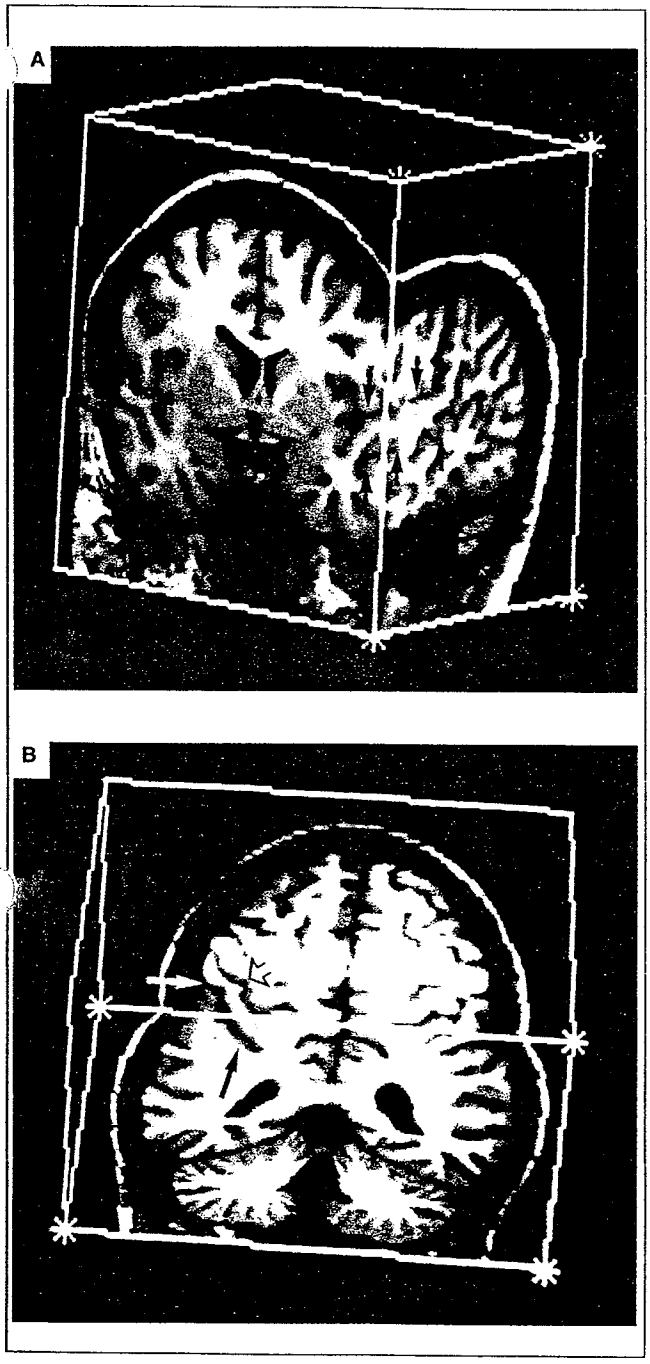

Figure 7. Application of the method for coordinate transformation to a 3D-FLASH MR image data set (TR 40 msec, TE 15 msec, flip angle 50°, slice thickness 3.1 mm). (A) Computer reformation of MR image data displaying coronal (left) and sagittal (right; anterior is left) planes simultaneously. The vertical line in the middle marks the intersection of the two planes and defines identical points in the cartesian coordinate system. A given spatial location in one plane can therefore be related to a location in the other plane. The arrows mark the sylvian fissure (above) and the superior temporal sulcus (below) in both planes. (B) Reformatted image displaying coronal (below) and transaxial (above; anterior is at the top) planes simultaneously. The line in the middle marks the intersection of the two planes and defines identical points in the cartesian coordinate system. The arrows mark the central (open arrow), and postcentral (solid arrows) sulci.

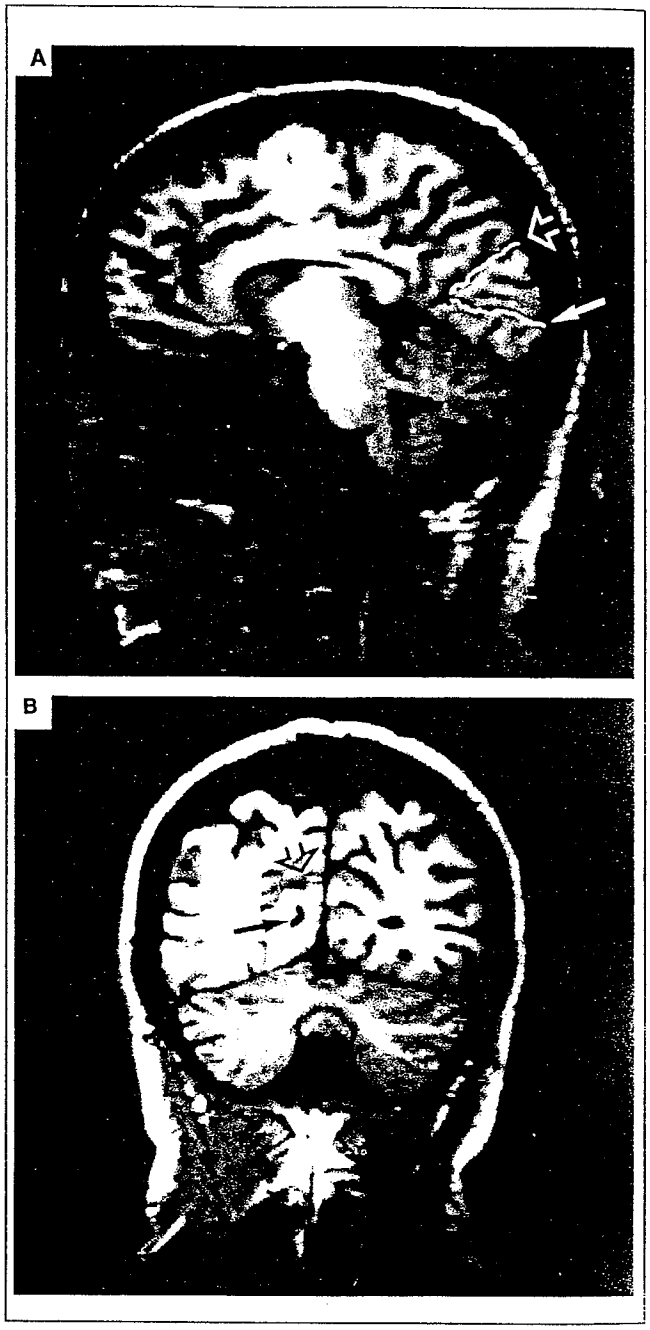

Figure 8. Topography of parietooccipital and posterior calcarine sulci: representative illustration of the application of the coordinate transformation method. (A) Identification of the cerebral sulci of interest in the plane of choice, in this case the paramedian sagittal plane, with subsequent digitization of the individual sulcal pattern. (Asterisk), cuneal point. (B) After application of the coordinate transformation the intersections of the sulcal outlines on a given coronal plane appear as small bars. The sulci, once identified and digitized in the sagittal (or transaxial) plane, can therefore be traced on coronal slices along their total anterior–posterior extent. (Open arrows), parietooccipital sulcus; (solid arrows), calcarine sulcus.

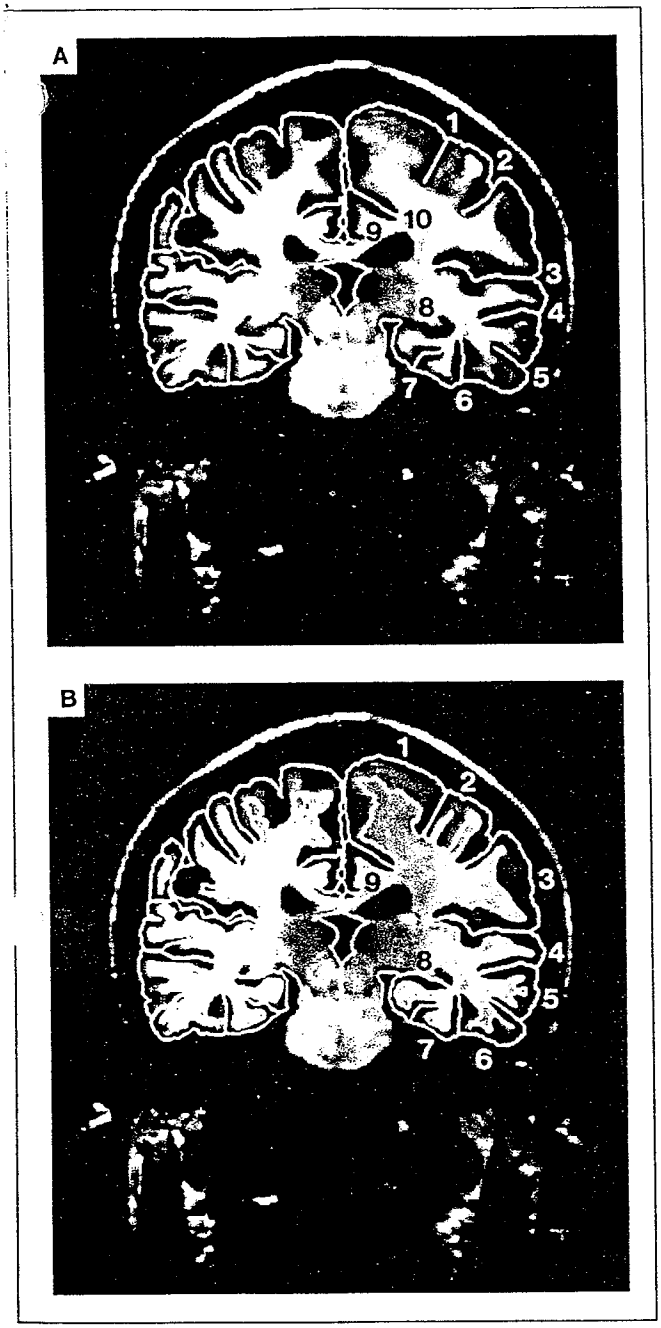

Figure 9. Topography of cerebral sulci and cortical parcellation units. (A) Coronal MRI section displaying the edited outlines of the intensity and differential contour algorithms, after application of the coordinate transformations and identification of the "limiting sulci." 1, Central sulcus; 2, postcentral sulcus; 3, sylvian fissure; 4, superior temporal sulcus; 5, inferior temporal sulcus; 6, occipitotemporal sulcus; 7, collateral sulcus; 8, hippocampal fissure; 9, callosal sulcus; 10, cingulate sulcus. (B) Same MRI section as in A after definition and digitization of the cortical parcellation units. 1, Precentral gyrus; 2, postcentral gyrus; 3, anterior supramarginal gyrus; 4, 5, 6, superior, middle, and inferior temporal gyri; 7, fusiform gyrus; 8, parahippocampal gyrus; 9, cingulate gyrus. The borders of the parietal operculum, Heschl's gyrus, and the planum temporale have yet to be digitized in our example and these regions are therefore still included in the supramarginal and superior temporal gyri, respectively.

sulci and additional coronal planes (Table 2 and Figs. 1 to 6). Both absolute volumes (cm^3) and proportional volumes (%) relative to the total cortical volume of each hemisphere were determined for the parcellation units (Table 4).

Acknowledgments

Dr. J. Rademacher, now at the Department of Neurology, Heinrich-Heine-University Düsseldorf, Moorenstr. 5, 4000 Düsseldorf 1, Germany, received a grant from the Deutsche Forschungsgemeinschaft.

Reprint requests should be sent to Dr. A. Galaburda, Beth Israel Hospital, 330 Brookline Ave., Boston, MA 02215 or Dr. Verne S. Caviness, Jr., Dept. of Neurology, MGH, 32 Fruit St., Boston, MA 02214.

REFERENCES

Albanese, E., Merlo, A., Albanese, A., & Gomez, E. (1989). Anterior speech region. Asymmetry and weight-surface correlation. *Archives of Neurology, 46,* 307–310.

Amaral, D. G., & Insausti, R. (1990). Hippocampal formation. In G. Paxinos (Ed.), *The human nervous system* (pp. 711–755). San Diego: Academic Press.

Bailey, P., & von Bonin, G. (1951). *The isocortex of man.* Urbana: University of Illinois Press.

Bajcsy, R., Lieberson, R., & Reivich, M. (1983). A computerized system for the elastic matching of deformed radiographic images to idealized atlas images. *Journal of Computer Assisted Tomography, 7,* 618–625.

Belliveau, J. W., Kennedy, D. N., McKinstry, R. C., Buchbinder, B. R., Weisskopf, R. M., Cohen, M. S., Vevea, J. M., Brady, T. J., & Rosen, B. R. (1992). Functional mapping of the human visual cortex by magnetic resonance imaging. *Science, 254,* 716–719.

Bogen, J. E., & Bogen, G. M. (1976). Wernicke's region—Where is it? *Annals of the New York Academy of Sciences, 280,* 834–843.

Bohm, C., Greitz, T., Kingsley, D., Berggren, B. M., & Olsson, L. (1983). Adjustable computerized stereotaxic brain atlas for transmission and emission tomography. *American Journal of Neuroradiology, 4,* 731–733.

Braak, H. (1980). *Architectonics of the human telencephalic cortex.* Berlin: Springer-Verlag.

Brockhaus, H. (1940). Die Cyto- und Myeloarchitektonik des Cortex claustralis und des Claustrum beim Menschen. *Journal für Psychologie und Neurologie, 49,* 249–348.

Brodmann, K. (1909). *Vergleichende Lokalisationslehre der Grosshirnrinde.* Leipzig: Barth.

Chollet, F., DiPiero, V., Wise, R. J. S., Brooks, D. J., Dolan, R. J., & Frackowiak, R. S. J. (1991). The functional anatomy of motor recovery after stroke in humans: A study with positron emission tomography. *Annals of Neurology, 29,* 63–71.

Clarke, S., & Miklossy, J. (1990). Occipital cortex in man: Organization of callosal connections, related myelo- and cytoarchitecture, and putative boundaries of functional visual areas. *Journal of Comparative Neurology, 298,* 188–214.

Corbetta, M., Miezin, F. M., Dobmeyer, S., Shulman, G. L., & Petersen, S. E. (1991). Selective and divided attention during visual discriminations of shape, color, and speed: Functional anatomy by positron emission tomography. *Journal of Neuroscience, 11,* 2383–2402.

Critchley, M. (1953). *The parietal lobe.* London: Edward Arnold.

Cunningham, D. J. (1892). *Contribution to the surface anatomy of the cerebral hemispheres.* Dublin: Royal Irish Academy.

Damasio, A. R. (1985). Disorders of complex visual processing: agnosias, achromatopsia, Balint's syndrome, and related difficulties of orientation and construction. In M.-M. Mesulam (Ed.), *Principles of behavioral neurology* (pp. 259–288). Philadelphia: F. A. Davis.

Damasio, H., & Damasio, A. R. (1989). *Lesion analysis in neuropsychology.* New York: Oxford University Press.

Dann, R., Hoford, J., Kovacic, S., Reivich, M., & Bajcsy, R. (1989). Evaluation of elastic matching system for anatomic (CT, MR) and functional (PET) cerebral images. *Journal of Computer Assisted Tomography, 13,* 603–611.

Duvernoy, H.M. (1988). *The human hippocampus.* München: J. F. Bergmann Verlag.

Eberstaller, O. (1890). *Das Stirnhirn. Ein Beitrag zur Anatomie der Oberfläche des Gehirns.* Wien-Leipzig: Urban & Schwarzenberg.

Eidelberg, D., & Galaburda, A. M. (1984). Inferior parietal lobule. Divergent architectonic asymmetries in the human brain. *Archives of Neurology, 41,* 843–852.

Evans, A. C., Beil, C., Marrett, S., Thompson, C. J., & Hakim, A. (1988). Anatomical-functional correlation using an adjustable MRI-based region of interest atlas with positron emission tomography. *Journal of Cerebral Blood Flow and Metabolism, 8,* 513–530.

Filimonoff, I. N. (1932). Über die Variabilität der Grosshirnrindenstruktur. Mitteilung II: Regio occipitalis beim erwachsenen Menschen. *Journal für Psychologie und Neurologie, 44,* 1–96.

Filipek, P. A., Kennedy, D. N., Caviness, V. S. Jr., Rossnick, S. L., Spraggins, T. A., & Starewicz, P. M. (1989). Magnetic resonance imaging-based brain morphometry: development and application to normal subjects. *Annals of Neurology, 25,* 61–67.

Flechsig, P. (1920). *Anatomie des menschlichen Gehirns und Rückenmarks auf myelogenetischer Grundlage.* Leipzig: Thieme.

Fox, P. T., Burton, H., & Raichle, M. E. (1987). Mapping human somatosensory cortex with positron emission tomography. *Journal of Neurosurgery, 67,* 34–43.

Fox, P. T., Mintun, M. A., Raichle, M. E., Miezin, F. M., Allman, J. M., & Van Essen, D. C. (1986). Mapping human visual cortex with positron emission tomography. *Nature (London), 323,* 806–809.

Fox, P. T., Perlmutter, J. S., & Raichle, M. E. (1985). A stereotactic method of anatomical localization for positron emission tomography. *Journal of Computer Assisted Tomography, 9,* 141–153.

Gado, M., Hanaway, J., & Frank, R. (1979). Functional anatomy of the cerebral cortex by computed tomography. *Journal of Computer Assisted Tomography, 3,* 1–19.

Galaburda, A. M. (1980). La région de Broca: observations anatomiques faites un siècle après la mort de son découvreur. *Revue Neurologique, 136,* 609–616.

Galaburda, A. M., Aboitiz, F., Rosen, G. D., & Sherman, G. F. (1985). Histologic asymmetries in the rat's primary visual cortex: implications for mechanisms of cerebral asymmetry. *Cortex, 22,* 151–160.

Galaburda, A. M., & Sanides, F. (1980). Cytoarchitectonic organization of the human auditory cortex. *Journal of Comparative Neurology, 190,* 597–610.

Galaburda, A. M., Sanides, F., & Geschwind, N. (1978). Human brain. Cytoarchitectonic left-right asymmetries in the temporal speech region. *Archives of Neurology, 35,* 812–817.

Galaburda, A. M., Sherman, G. F., Rosen, G. D., Aboitiz, F., & Geschwind, N. (1985). Developmental dyslexia: four consecutive patients with cortical anomalies. *Annals of Neurology, 18,* 222–233.

Gelbert, F., Bergvall, U., Salamon, G., Sobel, D., Jiddane, M., Corbaz, J.-M., & Morel, M. (1986). CT identification of cortical speech areas in the human brain. *Journal of Computer Assisted Tomography, 10,* 39–46.

Geschwind, N., & Galaburda, A. M. (1985). Cerebral lateralization. Biological mechanisms and pathology: I. A hypothesis and a program for research. *Archives of Neurology, 42,* 428–459.

Geschwind, N., & Levitsky, W. (1968). Human brain: Left-right asymmetries in temporal speech region. *Science, 161,* 186–187.

Goldman-Rakic, P. S., & Rakic, P. (1984). Experimental modification of gyral patterns. In N. Geschwind & A. M. Galaburda (Eds.), *Cerebral dominance. The biological foundations* (pp. 179–192). Cambridge, MA: Harvard University Press.

Greitz, T., Bohm, C., Holte, S., & Eriksson, L. (1991). A computerized brain atlas: construction, anatomical content, and some applications. *Journal of Computer Assisted Tomography, 15,* 26–38.

Habib, M., Renucci, R. L., Vanier, M., Corbaz, J. M., & Salamon, G. (1984). CT assessment of right-left asymmetries in the human cerebral cortex. *Journal of Computer Assisted Tomography, 8,* 922–927.

Hart, J. Jr., Lesser, R. P., Fischer, R. S., Schwerdt, P., Bryan, R. N., & Gordon, B. (1991). Dominant-side intracarotid amobarbital spares comprehension of word meaning. *Archives of Neurology, 48,* 55–58.

Huttenlocher, P. R. (1979). Synaptic density in human frontal cortex—developmental changes and effects of aging. *Brain Research, 163,* 195–205.

Jouandet, M. L., Tramo, M. J., Herron, D. M., Hermann, A., Loftus, W. C., Bazell, J., & Gazzaniga, M. S. (1989). Brainprints: Computer-generated two-dimensional maps of the human cerebral cortex in vivo. *Journal of Cognitive Neuroscience, 1*(1), 88–117.

Kaas, J. H., & Pons, T. P. (1988). The somatosensory system of primates. In H. P. Steklis & J. Erwin (Eds.), *Comparative primate biology* (pp. 421–468). New York: Alan R. Liss.

Kaas, J. H. (1990). Somatosensory system. In G. Paxinos (Ed.), *The human nervous system* (pp. 813–844). San Diego: Academic Press.

Kennedy, D. K., Filipek, P. A., & Caviness, V. S. Jr., (1989). Anatomic segmentation and volumetric calculation in cross-sectional magnetic resonance imaging. *IEEE Transactions on Medical Imaging, 8*(1), 1–7.

Kertesz, A., Black, S. E., Polk, M., & Howell, J. (1986). Cerebral asymmetries on magnetic resonance imaging. *Cortex, 22,* 117–127.

Kreht, H. (1936). Cytoarchitektonik und motorisches Sprachzentrum. *Zeitschrift für Mikroskopisch-Anatomische Forschung, 39,* 331–354.

Lang, J., & Belz, J. (1981). Form und Maße der Gyri und Sulci an der Facies superolateralis und Facies inferior hemispherii. *Journal für Hirnforschung, 22,* 517–533.

Lang, J., & Wachsmuth, W. (1985). *Praktische Anatomie: ein Lehr- und Hilfsbuch der anatomischen Grundlagen ärztlichen Handelns. Erster Band, Teil 1A.* Berlin: Springer-Verlag.

LeMay, M., & Kido, D. K. (1978). Asymmetries of the cerebral hemispheres on computed tomograms. *Journal of Computer Assisted Tomography, 2,* 471–476.

Livingstone, M., & Hubel, D. (1988). Segregation of form, color, movement, and depth: Anatomy, physiology, and perception. *Science, 240,* 740–749.

Lüders, H., Lesser, R. P., Hahn, J., Dinner, D. S., Morris, H.,

Resor, S., & Harrison, M. (1986). Basal temporal language area demonstrated by electrical stimulation. *Neurology, 36,* 505–510.

ers, H., Lesser, R. P., Hahn, J., Dinner, D. S., Morris, H. H., Wyllie, E., & Godoy, J. (1991). Basal temporal language area. *Brain, 114,* 743–754.

Marcotte, A. C., & Morere, D. A. (1990). Speech lateralization in deaf populations: evidence for a developmental critical period. *Brain and Language, 39,* 134–152.

Mazziotta, J. C., Phelps, M. E., Carson, R. E., & Kuhl, D. E. (1982). Tomographic mapping of human cerebral metabolism: Auditory stimulation. *Neurology, 32,* 921–937.

Mesulam, M.-M. (1985). Patterns in behavioral neuroanatomy: association areas, the limbic system, and hemispheric specialization. In M.-M. Mesulam (Ed.), *Principles of behavioral neurology* (pp. 1–70). Philadelphia: F. A. Davis.

Mesulam, M.-M. (1990). Large-scale neurocognitive networks and distributed processing for attention, language, and memory. *Annals of Neurology, 28,* 597–613.

Mesulam, M.-M., & Mufson, E. J. (1985). The insula of Reil in man and monkey. Architectonics, connectivity, and function. In A. Peters & E. G. Jones (Eds.), *Cerebral cortex* (pp. 179–226). New York: Plenum Press.

Mishkin, M., Ungerleider, L. G., & Macko, K. A. (1983). Object vision and spatial vision: two cortical pathways. *Trends in Neuroscience, 6,* 414–417.

Mohr, J. P., Pessin, M. S., Finkelstein, S., Funkenstein, H. H., Duncan, G. W., & Davis, K. R. (1978). Broca aphasia: Pathologic and clinical. *Neurology, 28,* 311–324.

Mountcastle, V. B. (1978). An organizing principle for cerebral function: The unit module and the distributed system. In G. M. Edelman & V. B. Mountcastle (Eds.), *The mindful brain* (pp. 7–50). Cambridge, MA: MIT Press.

Naidich, T. P., Daniels, D. L., Haughton, V. M., Williams, A., Pojunas, K., & Palacios, E. (1987). Hippocampal formation and related structures of the limbic lobe: anatomic-MR correlation. Part I. Surface features and coronal sections. *Radiology, 162,* 747–754.

Ojemann, G. A. (1979). Individual variability in cortical localization of language. *Journal of Neurosurgery, 50,* 164–169.

Ojemann, G. A. (1983). Brain organization for language from the perspective of electrical stimulation mapping. *The Behavioral and Brain Sciences, 6,* 189–206.

Ono, M., Kubik, S., & Abernathey, C. D. (1990). *Atlas of the cerebral sulci.* Stuttgart: Georg Thieme Verlag.

Pandya, D. N., & Yeterian, E. H. (1985). Architecture and connections of cortical association areas. In A. Peters & E. G. Jones (Eds.), *Cerebral cortex* (pp. 3–61). New York: Plenum Press.

Pelizzari, C. A., Chen, G. T. Y., Spelbring, D. R., Weichselbaum, R. R., & Chen, C.-T. (1989). Accurate three-dimensional registration of CT, PET, and/or MR images of the brain. *Journal of Computer Assisted Tomography, 13,* 20–26.

Penfield, W., & Rasmussen, T. (1950). *The cerebral cortex of man.* New York: Macmillan.

Perlmutter, J. S., Powers, W. J., Herscovitch, P., Fox, P. T., & Raichle, M. E. (1987). Regional asymmetries of cerebral blood flow, blood volume, and oxygen utilization and extraction in normal subjects. *Journal of Cerebral Blood Flow and Metabolism, 7,* 64–67.

Petersen, S. E., Fox, P. T., Posner, M. I., Mintun, M., & Raichle, M. E. (1988). Positron emission tomographic studies of the cortical anatomy of single-word processing. *Nature (London), 331,* 585–589.

Petersen, S. E., Fox, P. T., Snyder, A. Z., & Raichle, M. E. (1990). Activation of extrastriate and frontal cortical areas by visual words and word-like stimuli. *Science, 249,* 1041–1044.

Pfeifer, R. A. (1920). Myelogenetisch-anatomische Untersuchungen über das kortikale Ende der Hörleitung. *Abh math phys Kl sächs Akad Wiss, 37,* 1–54.

Pfeifer, R. A. (1936). Pathologie der Hörstrahlung und der corticalen Hörsphäre. In O. Bumke & O. Foerster (Eds.), *Handbuch der Neurologie* (Vol. 6, pp. 533–626). Berlin: Springer-Verlag.

Pieniadz, J. M., & Naeser, M. A. (1984). Computed tomographic scan cerebral asymmetries and morphologic brain asymmetries. Correlation in the same cases post mortem. *Archives of Neurology, 41,* 403–409.

Pietrzyk, U., Herholz, K., & Heiss, W.-D. (1990). Three-dimensional alignment of functional and morphological tomograms. *Journal of Computer Assisted Tomography, 14,* 51–59.

Posner, M. I., Petersen, S. E., Fox, P. T., & Raichle, M. E. (1988). Localization of cognitive operations in the human brain. *Science, 240,* 1627–1631.

Rademacher, J., Caviness, V. S. Jr., Steinmetz, H., & Galaburda, A. M. (1992). Topographical variation of the human primary cortices: Implications for neuroimaging and brain mapping studies. Submitted for publication.

Rakic, P. (1988). Specification of cerebral cortical areas. *Science, 241,* 170–176.

Rakic, P., Bourgeois, J.-P., Eckenhoff, M. F., Zecevic, N., & Goldman-Rakic, P. S. (1986). Concurrent overproduction of synapses in diverse regions of the primate cerebral cortex. *Science, 232,* 232–234.

Retzius, G. (1896). *Das Menschenhirn.* Stockholm: Norstedt & Söner.

Riegele, L. (1931). Die Cytoarchitektonik der Felder der Brocaschen Region. *Journal für Psychologie und Neurologie, 42,* 496–514.

Roland, P. E. (1984). Metabolic measurements of the working frontal cortex in man. *Trends in Neuroscience, 7,* 430–435.

Roland, P. E. (1985). Cortical organization of voluntary behavior in man. *Human Neurobiology, 4,* 155–167.

Rosen, G. D., Sherman, G. F., & Galaburda, A. M. (1989). Interhemispheric connections differ between symmetrical and asymmetrical brain regions. *Neuroscience, 33,* 525–533.

Rubens, A. B., Mahowald, M. W., & Hutton, J. T. (1976). Asymmetry of the lateral (sylvian) fissures in man. *Neurology, 26,* 620–624.

Sanides, F. (1962). *Die Architektonik des menschlichen Stirnhirns.* Berlin: Springer-Verlag.

Sarkisov, S. A. (1966). *The structure and functions of the brain.* Bloomington, IN: Indiana University Press.

Schulze, H. A. F. (1960). Zur individuellen cytoarchitektonischen Gestaltung der linken und rechten Hemisphäre im Bereiche des Lobulus parietalis inferior. *Journal für Hirnforschung, 4,* 486–517.

Seitz, R. J., Bohm, C., Greitz, T., Roland, P. E., Eriksson, L., Blomqvist, G., Rosenqvist, G., & Nordell, B. (1990). Accuracy and precision of the computerized brain atlas programme for localization and quantification in positron emission tomography. *Journal of Cerebral Blood Flow and Metabolism, 10,* 443–457.

Seltzer, B., & Pandya, D. N. (1980). Converging visual and somatic sensory cortical input to the intraparietal sulcus of the rhesus monkey. *Brain Research, 192,* 339–351.

Steinmetz, H., Ebeling, U., Huang, Y., & Kahn, T. (1990a). Sulcus topography of the parietal opercular region: an anatomic and MR study. *Brain and Language, 38,* 515–533.

Steinmetz, H., Fürst, G., & Freund, H.-J. (1989a). Cerebral cortical localization: application and validation of the proportional grid system in MR imaging. *Journal of Computer Assisted Tomography, 13,* 10–19.

Steinmetz, H., Fürst, G., & Freund, H.-J. (1990b). Variation of perisylvian and calcarine anatomic landmarks within stereotaxic proportional coordinates. *American Journal of Neuroradiology, 11,* 1123–1130.

Steinmetz, H., Rademacher, J., Huang, Y., Hefter, H., Zilles, K., Thron, A., & Freund, H.-J. (1989b). Cerebral asymmetry: MR planimetry of the human planum temporale. *Journal of Computer Assisted Tomography, 13,* 996–1005.

Steinmetz, H., Rademacher, J., Jäncke, L., Huang, Y., Thron, A., & Zilles, K. (1990c). Total surface of temporoparietal intrasylvian cortex: diverging left-right asymmetries. *Brain and Language, 39,* 357–372.

Steinmetz, H., Volkmann, J., Jäncke, L., & Freund, H.-J. (1991). Anatomical left-right asymmetry of language-related temporal cortex is different in left- and right-handers. *Annals of Neurology, 29,* 315–319.

Stensaas, S. S., Eddington, D. K., & Dobelle, W. H. (1974). The topography and variability of the primary visual cortex in man. *Journal of Neurosurgery, 40,* 747–755.

Strasburger, E. H. (1938). Vergleichende myeloarchitektonische Studien an der erweiterten Brocaschen Region des Menschen. *Journal für Psychologie und Neurologie, 48,* 477–511.

Talairach, J., Szikla, G., Tournoux, P., Prosalentis, A., Bordas-Ferrier, M., Covello, L., Iacob, M., & Mempel, E. (1967). *Atlas d'Anatomie Stéréotaxique du Télencephale.* Paris: Masson.

Van Essen, D. C. (1985). Functional organization of primate visual cortex. In A. Peters & E. G. Jones (Eds.), *Cerebral cortex* (pp. 259–329). London: Plenum Press.

Van Hoesen, G. W. (1982). The primate parahippocampal gyrus: New insights regarding its cortical connections. *Trends in Neuroscience, 5,* 345–350.

von Economo, C., & Horn, L. (1930). Über Windungsrelief, Maße und Rindenarchitektonik der Supratemporalfläche, ihre individuellen und ihre Seitenunterschiede. *Zeitschrift für Neurologie und Psychiatrie, 130,* 678–757.

von Economo, C., & Koskinas, G. N. (1925). *Die Cytoarchitektonik der Hirnrinde des erwachsenen Menschen.* Berlin: Springer-Verlag.

Wada, J. A., Clarke, R., & Hamm, A. (1975). Cerebral hemisphere asymmetry in humans. *Archives of Neurology, 32,* 239–246.

Wise, R., Chollet, F., Hadar, U., Friston, K., Hoffner, E., & Frackowiak, R. (1991). Distribution of cortical neural networks involved in word comprehension and word retrieval. *Brain, 114,* 1803–1817.

Wise, S. P., & Strick, P. L. (1984). Anatomical and physiological organization of the non-primary motor cortex. *Trends in Neuroscience, 7,* 442–446.

Witelson, S. F., & Kigar, D. L. (1988). Asymmetry in brain function follows asymmetry in anatomical form: gross, microscopic, postmortem and imaging studies. In F. Boller, J. Grafman, G. Rizzolatti, & H. Goodglass (Eds.), *Handbook of Neuropsychology.* New York: Elsevier Science Publishers.

Woolsey, C. N., Erickson, T. C., & Gilson, W. E. (1979). Localization in somatic sensory and motor areas of human cerebral cortex as determined by direct recording of evoked potentials and electric stimulation. *Journal of Neurosurgery, 51,* 476–506.

Zeki, S. M. (1978). Functional specialization in the visual cortex of the rhesus monkey. *Nature (London), 274,* 423–428.

Zeki, S. (1990). A century of cerebral achromatopsia. *Brain, 113,* 1721–1777.

Zihl, J., von Cramon, D., Mai, N., & Schmid, C. (1991). Disturbance of movement vision after bilateral posterior brain damage. *Brain, 114,* 2235–2252.

Zilles, K. (1990). Cortex. In G. Paxinos (Ed.), *The human nervous system* (pp. 757–802). San Diego: Academic Press.

Zilles, K., Armstrong, E., Schleicher, A., & Kretschmann, H.-J. (1988). The human pattern of gyrification in the cerebral cortex. *Anatomy and Embryology, 179,* 173–179.